Recent developments in the detection of bovine serum albumin

Ali Jahanban-Esfahlan, Alireza Ostadrahimi, Rana Jahanban-Esfahlan, Leila Roufegarinejad, Mahnaz Tabibiazar, Ryszard Amarowicz

PII: S0141-8130(19)33408-7
DOI: https://doi.org/10.1016/j.ijbiomac.2019.07.096
Reference: BIOMAC 12848

To appear in: *International Journal of Biological Macromolecules*

Received date: 8 May 2019
Revised date: 13 July 2019
Accepted date: 13 July 2019

Please cite this article as: A. Jahanban-Esfahlan, A. Ostadrahimi, R. Jahanban-Esfahlan, et al., Recent developments in the detection of bovine serum albumin, International Journal of Biological Macromolecules, https://doi.org/10.1016/j.ijbiomac.2019.07.096

Recent Developments in the Detection of Bovine Serum Albumin

Ali Jahanban-Esfahlan[a,b,c*], Alireza Ostadrahimi[a], Rana Jahanban-Esfahlan[d]

Leila Roufegarinejad[e], Mahnaz Tabibiazar[a], , Ryszard Amarowicz[f]

[a] Nutrition Research Center, Tabriz University of Medical Sciences, Tabriz, Iran

[b] Student Research Committee, Tabriz University of Medical Sciences, Tabriz, Iran

[c] Infectious and Tropical Diseases Research Center, Tabriz University of Medical Sciences, Tabriz, Iran

[d] Department of Medical Biotechnology, School of Advanced Medical Scieces, Tabriz University of Medical Sciences, Tabriz, Iran

[e] Department of Food Sciences, Tabriz branch, Islamic Azad University, Tabriz, Iran

[f] Division of Food Sciences, Institute of Animal Reproduction and Food Research of the Polish Academy of Sciences, Olsztyn, Poland

[*]Corresponding author: Ali Jahanban-Esfahlan, Daneshghah Street, Student Research Committee, Tabriz University of Medical Sciences, Tabriz, Iran, Tel: + 98 41 33366581, Fax: + 98 41 33366581, E-mail address: a.jahanban@gmail.com.

Table of Contents

Abstract 4
Keywords: 4
Abbreviations 5
1. Introduction 6
2. Serum Albumins 7
2.1. HSA 8
2.2. BSA 9
3. Determination of BSA 9
3.1. BSA quantification by CE 10
3.2. BSA recognition using fluorescent materials 12
3.2.1. Fluorescent probes 13
3.2.1.1. Diketopyrrolopyrrole and its derivatives 13
3.2.1.2. Chemically converted graphene (CCG)-dye complexes 15
3.2.1.3. Dye-metal complexes 16
3.2.1.4. Other fluorescent probes 18
3.2.2. Fluorescence resonance energy transfer (FRET) 20
4. Nanomaterial-based sensors 22
4.1. Magnetic nanoparticles (MNPs) 22
4.2. Nanomaterials based on Gold 22
4.2.1. AuNPs 22
4.2.2. Gold nanorods (Au NRs) 24
4.3. Nanomaterials based on Zinc oxide (ZnO) 25
4.3.1. Zinc oxide microwires 25
4.3.2. ZnO nanospheres 25
4.3.3. Al_2O_3/ZnO nanolaminates 26
4.4. Nanomaterials based on silver 26
4.4.1. Silver nanoparticles (AgNPs) 26
4.4.2. TAgNPs 27
4.4.3. Silver nanostructures (AgNSs) 28
4.5. GO-based nanomaterials 29
4.6. Carbon nanotubes 29
4.7. QDs 30
5. Other related works of interest 32
6. Conclusions 35

Conflict of interest 35
Acknowledgments 35
References 36
Figure captions 46

Abstract

Albumin is a globular protein which plays a pivotal role in maintaining plasma pressure and the nutritional balance. Different compounds are transported by binding to albumin in the blood. Also, human health is closely related to the serum albumin concentration in blood plasma or other biological fluids. Due to the high structural similarity with human serum albumin (HSA), bovine serum albumin (BSA) has been widely investigated as a model protein in different fields. Importantly, albumin detection has recently gained huge interest, as this protein serves as an important indicator of cow health, and its milk and meat quality. Also, it is also known as an allergenic and a carrier protein. As a result, it is highly essential to determine bovine albumin in various industries, such as medicine, pharmaceutical, clinical and food. Therefore, the development of new, efficient, fast and straightforward methods for selective detection of BSA is critical. This review seeks to highlight different characteristics of BSA and its importance. Then, by focusing on recent developments made in the last two decades in BSA biosensing and determination methods, the use of different biomaterials/ nanomaterials is discussed.

Keywords:

Albumin; Biosensor; BSA; Interaction; Nanotechnology; Nanoparticles; Protein

Abbreviations

1D	One-dimensional
2D	Two-dimensional
3D	Three-dimensional
ACQ	Aggregation-caused quenching
Ag NPs	Silver nanoparticles
Ag_2SNPs	Silver sulphide nanoparticles
AgNSs	Silver nanostructures
AIE	Aggregation-induced emission
Al	Aluminium
AO	Acridine orange
APS	3-Aminopropyltrimethoxysilane
APTES	(3-Aminopropyl) triethoxysilane
AQ	9, 10-anthraquinone
ATRP	Atomic transfer radical polymerization
Au NRs	Gold nanorods
AuNPs	Gold nanoparticles
BDD	Boron-doped diamond
BR	Britton–Robison buffer
BRDVD	Blu-ray digital versatile disc
BSA	Bovine Serum Albumin
CAuNPs	Citrate-capped Au nanoparticles
CCG	Chemically converted graphene
CD	Circular dichroism
CdTe QDs	Cadmium telluride quantum dots
CE	Carbon electrode
CE	Capillary electrophoresis
CIHARP	4-Chloro-(2'-hydroxylophenylazo) rhodanine
CS	Chitosan
ctDNA	Calf thymus DNA
Cy3	Cyanin 3
Cys	Cysteine
CZE	Capillary zone electrophoresis
DEP	Dielectrophoresis
DISA	2,4-dihydroxyl-3-iodo salicylaldehyde azine
DPP	1,4-diketo-3,6-diphenylpyrrolo[3,4-c] pyrrole
ECL	Electrochemiluminescence
EDC	1-Ethyl-3-(3-dimethylaminopropyl)carbodiimide
EIS	Electrochemical impedance spectroscopy
ELISA	enzyme-linked immunosorbent assay
EMIPs	Epitope-based molecular imprinting polymers
ENX	Enoxacin
FDA	Food and drug administration
FET	Field effect transistors
FRET	Fluorescence resonance energy transfer
GE	Gold electrode
GE	Gel electrophoresis
GMR	Guided mode resonance
GO	Graphene oxide
H-bonding	Hydrogen bonding
HCPT	10-Hydroxy camptothecin
HPLC	High performance liquid chromatography
HSA	Human serum albumin
ITO	Indium tin oxide
LbL	Layer-by-layer
LIF	Laser-induced fluorescence
LOD	Limit of detection
LSPR	Localized surface plasmon resonance
MIMs	Molecularly imprinted membrane
MIPs	Molecularly imprinted polymers
MNPs	Magnetic nanoparticles
MoS_2	Molybdenum disulphide
MWCNTs	Multi-walled carbon nanotubes
NIR	Near-infrared
NIRDRS	Near-infrared diffuse reflectance spectroscopy
NPs	Nanoparticles
NR	Neutral red
OLEDs	Organic light-emitting diodes
PDAs	Polydiacetylenes
Phe	Phenylalanine
PSCs	Polymer solar cells
QCI	Quartz crystal impedance
QDIC	Quasi-digital impedance converter
R6G	Rhodamine-6G
RLS	Resonance light scattering
SERS	Surface-enhanced Raman scattering
SPR	Surface plasmon resonance
SQ	Squaraine
TAgNPs	Triangular silver nanoplates
TGA	Thioglycolic acid
THF	Tetrahydrofuran
Ti	Titanium
TIRE	Total internal reflection ellipsometry
TMA	Trimethylamine

Trp	Tryptophan	ZnO	Zinc oxide
Ts	Substrate temperature	$ZnO-NH_2$	NH_2-functionalized zinc oxide
Tyr	Tyrosine	λ_{max}	Maximum absorption wavelength
UV	Ultra violet		
UV–vis	Ultra violet-visible		

1. Introduction

Since proteins perform a myriad of functions such as transporter, building blocks, and pathogens in biology, the recognition of these macromolecules is essential [1]. For biological studies and clinical diagnosis, the detection and determination of different proteins is of great

importance, requiring highly sensitive and selective detection methods. It is necessary to determine the amounts of albumin protein in biochemistry, pathology, and clinical diagnosis, as it is often used to quantify other constituents in living systems. Different methods are used to determine protein concentration, including Biuret method, Lowry method, Bradford method and Bromocresol Green method [2]. However, these methods suffer from several constraints such as dynamic range, limited sensitivity, sample treatment or unsatisfactory detection limit. The low sensitivity and selectivity, as well as the complicated measurement stages, are the significant disadvantages of the Lowry method. Also, a poor linearity between the protein concentration and the dye absorbance of Coomassie Brilliant Blue G-250-protein complex and the operational troubles are the main problems of the Bradford method. Likewise, the Bromocresol Green method is susceptible to turbidity disruption and is not sufficiently sensitive to trace analysis [3]. Today, these limitations are attempted to be overcome by developing new methods.

Experimental biochemical assays are commonly used to determine albumin concentration because the amount of this macromolecule has a significant effect on the biological systems. Hence, the development of fast, simple and highly sensitive diagnostic methods is required for the accurate analysis of albumin in biological samples/fluids.

Herein, we first overview albumin structure and highlight the significance of its detection. Then, recent trends in BSA recognition and biosensing using different biomaterials/nanomaterials are presented.

2. Serum Albumins

Serum albumins are the most abundant (52-62%) total water-soluble fraction proteins in the blood plasma [4, 5]. Generally, they have a single polypeptide chain composed of ~585 amino acid residues. Circulatory, nutritional and physiological functions of serum albumins make them as essential bio-macromolecules acting as a transporter for carrying, distributing and delivering different exogenous or endogenous substances, ions, fatty acids, small molecules such as pharmaceuticals in the body [4]. HSA and BSA are the most appreciated serum albumins used in different research fields.

2.1. HSA

HSA is the main protein present abundantly in the human blood circulatory system. It is a globular single chain polypeptide with the molecular weight of 66.8 kDa [6-8]. The structure of this heart-shaped protein is composed of 586 amino acids folding in 3 dimensions (3D) structure with three homologous domains (I, II and III), each domain containing two subdomains called subdomains A and B (Figure 1). There are two main binding sites on albumin which are commonly known as Sulow's sites I and II or the binding sites I and II positioned in the subdomains IIA and IIIA, respectively. Most of the small molecules and therapeutic chemicals have been reported to bind to these regions of albumin, but recently, other sites are recognized for the binding of such molecules to HSA, as well [9-12]. HSA has a wide range of physiological functions related to the binding, transport, and delivery of steroids, fatty acids, bilirubin, porphyrins, etc. [9]. Importantly, special focus has been placed on the development and fabrication of albumin-based nanoparticles (NPs) for the efficient delivery of various substances/biomolecules to target cells/organs. Such that, Abraxane can be considered as the characteristic example of albumin-based NPs approved in 2005 by the U.S. Food and Drug Administration (FDA). It was developed to surmount the low water solubility problem of anticancer agent paclitaxel with the mean particle size of 130 nm. The

formulation of Abraxane is mainly used for the treatment of patients suffering from metastatic breast cancers [13].

2.2. BSA

As BSA structure is very similar to HSA, it has been widely used as a model protein instead of HSA. Similar to HSA, BSA is composed of a single polypeptide chain which includes 583 amino acids residues [14]. The cross-linked 17 disulphide bridges of cysteine (Cys) amino acid residues stabilize the structure. Its molecular weight is approximately 66.8 kDa, and the heart-shaped structure has three homologous domains I-III and each domain consists of two subdomains, A and B, with unique binding properties [6]. In the subdomain IB and subdomain IIA, BSA contains two Tryptophan (Trp) amino acid residues as Trp-134 and Trp-212, respectively [4].

3. Determination of BSA

In the sense of medical applications and enzymatic reactions, BSA has many uses, as it is used as a protein reagent to measure the concentration of a protein in a solution, such as the Bradford test. BSA is also used as a standard protein in the design of new immunochemical tests. Moreover, albumin can be consumed as a dietary protein [15, 16]. The method for protein analysis should be accurate, fast, sensitive and reproducible. There are currently very sensitive methods for the detection and determination of BSA concentration, including electrochemical impedance spectroscopy, near-infrared diffuse reflectance spectroscopy, capillary electrophoresis (CE), and light scattering technique. Although these approaches have reasonable selectivity and sensitivity, they suffer of several disadvantages such as the incorrect results, the complexity of the procedure, poorly reproducible and time-consuming.

Therefore, the detection of minimal amounts of bovine albumin in the shortest time, using a biosensing tool with simple design and a high precision, is very desirable and is now under active research.

3.1. BSA quantification by CE

Decades ago, CE was utilized for the establishment of a fast and sensitive method for BSA quantification. Back then, a highly sensitive laser-induced fluorescence (LIF) scheme for the detection of native, Trp or Tyrosine (Tyr)-containing proteins by CE method was demonstrated in 1992 [17]. Hopefully, the presence of aromatic amino acids including, Trp, Tyr and Phenylalanine (Phe) in the structure of proteins has enabled the development of different fluorescent-based techniques with an acceptable limit of detection (LOD) [4]. It is worth to mention that in analytical chemistry, the lowest quantity of a substance is defined as LOD, the detection limit, or the lower limit of detection, which is distinguished from the absence of that substance as a blank value at a specified confidence level (commonly 99%). [18]. Accordingly, in this study the wavelength of 275.4 nm was used from an argon-ion laser source for exciting the intrinsic fluorescence of proteins, which recorded LOD of 1×10^{-10} M for conalbumin showing a 140-fold enhancement in the fluorescence intensity. With stacking at injection, the LOD was recorded to be 3×10^{-12} M. Linear dynamic ranges of at least 5 and 4 orders of magnitude were reported for Trp and BSA, respectively. Additional merits of the CE-LIF detecting platform include the design of a simply assembled, effective performance, compact, rugged and user-friendly design.

In another study, Pande, Nellore and Bhagat [19] tried to optimize and validate a reproducible, accurate and quick CE method for BSA assay. The effects of different factors such as the concentration of buffer, pH, capillary dimensions, additives such as surfactants

and proteins, solubilizers and the use of coated capillaries were considered. The additives or thin coatings gave no advantage in reducing BSA's surface adsorption on the capillary walls. Borate buffer with the concentration of 150 mM and pH 8.5, a 27 cm capillary with an aperture window of 100 × 200 μm represented the optimal detection conditions reported for the proposed method. At BSA concentrations of 25-1000 μg/ml, the validated BSA detection method for the inter-day and intraday variation coefficient was not greater than 7.59%.

As an additional technique for protein analysis, gel electrophoresis (GE), shows some drawbacks of being labor-intensive, time-consuming, and unsuitable for the quantification of various protein samples. For the rapid separation and analysis of charged molecules such as proteins and peptides, capillary zone electrophoresis (CZE) has been recommended as a compelling novel technique to address the problems associated with the GE method. As proof of principle, CZE equipped with a carbon fiber micro disk array electrode was employed to BSA analysis in bovine serum samples using an end-column amperometric detector [20]. In this research, the optimum conditions for separation and detection of BSA were 0.025 mol/l KH_2P0_4, 0.02 mol/l NaOH as a buffer solution, 20 kV, 5 kV and 10 s as separation voltage, injection voltage and the injection time, respectively and 0.90 V vs. SCE for the potential of detection. The obtained LOD was reported to be $4 \times l0^{-7}$ mol/l (0.7 fmol).

Recently, an automated Western blot called Simple Western based on CE was also described. This CE-based Western offers the advantages of fully automated operation except for sample preparation and a coefficient variation of below 10% compared to the standard enzyme-linked immunosorbent assay (ELISA) technique [21]. To analyze and detect the amounts of residual BSA in an attenuated virus vaccine, Loughney, Lancaster, Ha and Rustandi [22] reported the use of SimpleWestern technology to develop a novel improved method. The

method is based on automated Capillary Western and had two logs linearity, >80% spike recovery or precision, intermediate accuracy of variation coefficient <15%, and the quantitation limit of 5.2 ng/ml. The developed method was then used to determine BSA concentration in four lots of bulk vaccine products and was used to monitor the clearance of BSA during the purification process of the vaccine.

3.2. BSA recognition using fluorescent materials

The emission of the absorbed light or other electromagnetic radiation by a material is known as fluorescence. In most samples, the emission light goes to a higher wavelength, and hence its energy is lower than that the absorbed light radiation. The most remarkable instance of fluorescence happens when the absorbed light is in the ultraviolet range of the spectrum, and thus is not visible by the human eye, but the emission light is in the visible region, which produces a distinct color for fluorescent material [23]. It has been shown that different organic, inorganic or organometallic substances can exhibit fluorescence properties. Aromatic hydrocarbons (naphthalene, anthracene, phenanthrene, pyrene, perylene, etc.), fluorescein, rhodamines, coumarins, oxazines, polyenes, diphenylpolyenes, amino acids (Trp, Tyr, Phe), etc. are the main types of organic compounds, while uranyl ion (UO^{+2}), lanthanide ions (e.g. Eu^{3+},Tb^{3+}), doped glasses (e.g. with Nd, Mn, Ce, Sn, Cu, Ag), crystals (ZnS, CdS, ZnSe, CdSe, GaS, GaP, Al_2O_3/Cr^{3+} (ruby)), etc. are known as the inorganic fluorescence substances. Organometallic compounds include ruthenium complexes (e.g. Ru $(biPy)_3$), complexes with lanthanide ions, complexes with fluorogenic chelating agents (e.g. 8-hydroxyquinoline, also called oxine), etc. [24]. In fluorescence spectroscopy, the fluorescence resulting from a sample is analysed. Being fast, practical, highly sensitive and selective renders fluorescence technique a desirable detecting method than others. Likewise,

this technique is the most useful method for studying biomolecular interactions, as it is sensitive to low concentrations and friendly to the physiological environment [23].

3.2.1. Fluorescent probes

3.2.1.1. Diketopyrrolopyrrole and its derivatives

In aqueous solution with neutral pH, the isoelectric point of BSA is about 4.7. Thus, it is known as an acidic protein with the negative charges located in hydrophobic pockets inside the molecule [25]. Consequently, some dyes containing cationic groups such as ammonium and imidazolium can form aggregates induced by BSA through electrostatic and hydrophobic interactions. Based on these mechanisms and by utilizing the variations in their photophysical properties, different fluorescent bioprobes for BSA assay have been recently developed [26-29]. Commonly, when the traditional fluorescent dyes are in aqueous media or bound to analytes in high concentration, they exhibit aggregation-caused quenching (ACQ) behaviors. For the first time, aggregation-induced emission (AIE) as a unique photophysical phenomenon has been described by Wang, Qian, Qin, Qin, Tang and He [30]. Then, a wide variety of fluorescent 'light-up' sensors have been developed based on the AIE mechanism [31-40]. However, since the emission wavelength of most AIE-active probes induced by analytes is usually located in the Ultraviolet-visible (UV-vis) region, their application in *in vivo* imaging is limited.

Due to excellent red and strongly fluorescent emission and brilliant light, weather, and heat stability,1,4-diketo-3,6-diphenylpyrrolo[3,4-c] pyrrole (DPP) and its derivatives have been extensively used in the fabrication of polymer solar cells (PSCs) [41-44], organic light-emitting diodes (OLEDs) [45], field effect transistors (FET) [46-48], fluorescent probes [49-

56], two-photon absorption [57-59], and dye sensitizing solar cell applications [60-65]. DPP derivatives functionalized with electron-donating methoxytriphenylamine groups were AIE-active and can exhibit red to near-infrared (NIR) emission and significant Stokes shift, which can be advantageous in biological applications [66].

In this way, a new NIR emissive fluorophore DPPAM dye based on DPP molecule with ammonium groups as bioprobe and cell staining has been developed by Hang, Yang, Qu and Hua [67]. It was shown that this bioprobe was 'turn-on' response for BSA with high sensitivity and the NIR of its emission ranged from 600 to 850 nm. AIE-assisted bioimaging also exhibited the clear NIR signals in some special region where the dye-aggregates attached. The synthesis of the target compound DPPAM is shown in Figure 2A. In the first step, 1, 4-dibromobutane was attached to the core of DPP to form compound 2. Then, it was followed by Suzuki's palladium-mediated cross-coupling reaction between compound 2 and 4-(bis (4-methoxyphenyl)-amino) phenylboronic acid [Pd (PPh_3)$_4$], to produce compound 3. The treatment of compound 3 with trimethylamine (TMA) in anhydrous tetrahydrofuran (THF) subsequently resulted in DPPAM. The synthesized DPPAM is nearly nonemissive in aqueous solution, but it shows AIE-active properties and its sharp increase in NIR emissions around 703 nm is due to the aggregation and the complexation of DPPAM ammonium groups with BSA stabilizing by electrostatic interactions (Figure 2B). This DPPAM can be used as a fluorescent light-up bioprobe for the successful detection of BSA. Besides, the introduction of ammonium groups has improved the water solubility of the DPPAM, which has increased its application in bioimaging.

In another study, the fluorescence properties of two new synthesized DPP-based compounds were investigated, where *p*-cyanobenzaldehyde was used as starting material, and 2,5-dioctyl-

3,6-bis (4'-formylphenyl) pyrrolo[3,4-c] pyrrole-1,4-dione (compound 5) was prepared in five steps (Figure 3). The quaternization of compound 5 was used to produce the salt of DPP2 with trimethylamine, and the reaction of diethylamine with compound 5 gave DPP1 bioprobe. In this study, DPP1 with two diethylamino groups had a specific AIE property. That, under alkaline conditions DPP1 begins to aggregate due to the AIE effect and the chemical reactivity of the diethylamino group to H^+ ions (pH= 10.59). This is confirmed by the observation that at pH 12.36, the DPP1 emission intensity was 6.67 times higher than that at pH 2.53 indicating the fluorescent pH sensor function of DPP1. Meanwhile, given that DPP2 is an ammonium compound in the form of salt, it showed no AIE activity in solution. However, in a solid state, its emission showed considerable enhancement when the viscosity of the system is increased. Accordingly, in the presence of albumin, DPP2 can bind strongly to BSA, and thus, its fluorescence emission enhancement amplifies with 7.65-fold. Therefore, for the detection of BSA, DPP2 could be considered as a "turn on" biological fluorescent probe. As in cellular imaging of HeLa cells treated with DPP2, the appearance of red fluorescence in the cytoplasm of the cells indicated the application of DPP2 as a fluorescent probe because of its low cytotoxicity [68].

3.2.1.2. Chemically converted graphene (CCG)-dye complexes

Over the last hundred years, cyanins as classical dyes are widely used in the determination of amino acids, protein research, as well as the identification of cancer cells, among others [69]. Since CCG sheets are negatively charged in aqueous dispersion, organic molecules bearing positive charge can be absorbed via weak interactions such as electrostatic and π-π stacking

on the surface of CCG. The positively charged Cyanin 3 (Cy3) dye is a suitable candidate for strong noncovalent binding to the CCG with a negative charge (Figure 4). In aqueous solution, CCG could effectively quench the fluorescence emission of Cy3, and thus, the emission intensity was reduced to 1/38 of 1 alone, because of the hybrid formation between CCG and dye. CCG was synthesized using hydrazine hydrate with partial reduction of graphene oxide (GO) to remove oxygen atoms which restored the extent of aromatic double-bonded carbons and forms a colloidal dispersion. In the presence of a certain amount of BSA, the observed fluorescence intensity enhancement for the CCG–Cy3 hybrid system was about 60 times, rendering it highly applicable for the discrimination of BSA. The recorded fluorescence emission intensity was proportional to the concentration of added BSA in the range of 0 to 8×10^{-6} M, and the LOD of BSA was reported to be 5×10^{-8} M [70].

Squaraine (SQ) is one of the most appealing dyes, owing to it's the positive charge which represents a strong absorption and fluorescence spectra characteristics in the red to near-infrared region. Its chemical structure is illustrated in Figure 5A. CCG was reported to significantly increase the fluorescence intensity of SQ dyes in the presence of BSA. Though in absence of CCG a weak response of SQ towards BSA is reported, 80 fold enhancement in the fluorescence turn-on intensity can be obtained upon the addition of BSA to the solution of SQ–CCG aggregate affording quantification of bovine albumin [71].

3.2.1.3. Dye-metal complexes

The complex of dye probe and metal has advantages in terms of high sensitivity and selectivity compared to the metal ion or dye probe alone. Consequently, quantitative analysis method based on the complex formation between protein and dye-metal probe is rapidly developed. However, several limitations such as poor photostability, lower excited state

lifetime and absorption wavelength hindered the broad applications of organic fluorophores. As an additional limitation, the fluorescence spectra of the molecule as a probe compound should not overlap with the fluorescence spectra region of proteins. In this respect, the use of transition metal complexes with luminescent attributes as sensors attracted considerable attention because they exhibit a high absorption wavelength and long lifetime in comparison to the corresponding pure organic. Correspondingly, luminescent transition-metal complexes of rhenium (I), ruthenium (II), and osmium (II) with d^6 electronic configurations have increasing applied in imaging of biomolecules and development of luminescent probes. The complexes of ruthenium (II)-polypyridine represent advantages such as long-lived luminescence, high photostability, and low-energy absorption [72]. In this context, Babu, Mareeswaran, Singaravadivel, Bhuvaneswari and Rajagopal [73] described a luminescence sensor using two deep-red emissive ruthenium (II)-polypyridine complexes for the detection of BSA showing particular label-free properties. The chemical structures of both complexes are shown in Figure 5B. In this investigation, interactions between BSA and ruthenium (II) complexes were explored using spectroscopic techniques such as fluorescence emission, excited state lifetime, Ultraviolet (UV) absorption and circular dichroism (CD) spectroscopy. The detection of albumin was based on the enhanced luminescence intensity of both ruthenium (II) complexes (I and II) at 602 and 613 nm with a considerable hypsochromic shift of 18 and 5 nm, respectively, in the presence of BSA. Meanwhile, the high affinity of the probes to bind BSA and hydrophobic interactions were the main forces stabilizing the formed complexes. Based upon the calculated values for binding constant, the strong binding of the complex I compared to complex II was deducted to be related to the high hydrophobicity of complex I.

Rhodanine is a high-value reagent and is mainly used in the determination of metal ions and the spectroscopic determination of proteins. 4-chloro-(2'-hydroxylophenylazo) rhodanine-Titanium (IV) [CIHARP–Ti (IV)] complex as a fluorescence probe was used in a novel developed method for the determination of four types of proteins, including BSA, HSA, ovalbumin, and γ-globin under optimal conditions. The chemical structure of CIHARP is represented in Figure 5C, which is reported to display the wavelengths of excitation and emission of 335 nm and 376 nm, respectively. Detection was based on the enhancement of fluorescence, and in the presence of bis (2-ethylhexyl) sulfosuccinate sodium salt microemulsion, the sensitivity of the system was significantly increased, with LOD of 0.182 mg/ml for BSA and 0.0788 mg/ml for HAS, respectively. Also, the linear calibration was in the range of 0–12.0 and 0–10.0 mg/ml, respectively. Further, this method showed satisfactory results when applied for analysis of protein in cornmeal and milk powder with good selectivity and high sensitivity [74].

3.2.1.4. Other fluorescent probes

The improvement of photochemical reactivity can be used with a simple *In situ* photochemical kinetic fluorimetric method for the sensitive detection of labeled BSA. In an earlier study, labeling BSA with 9, 10-anthraquinone (AQ) (Figure 5D) showed a considerable improvement in its photochemical fluorimetric activity compared to free AQ. Further studding the spectral characteristics of the conjugated AQ photoreduction product revealed significant blue shifts in the excitation and emission bands in comparison with those of free AQ. The calibration graph was a linear range over the 0-l.8 × 10^{-7} M for BSA determination with the LOD of 1.2× 10^{-10} M [75].

In other experiments, nile blue (Figure 5E) as a cationic dye with a rigid and planar structure was used as a ligand to bind BSA molecule (635nm excitation, and 670 nm emission). The enhancement of Nile blue fluorescence at 670 nm was used for the development of a new fluorimetric technique for the determination of BSA concentrations at the microgram level. The method is based on the binding of Nile blue to BSA and producing a stable complex which is soluble in water. Moreover, the addition of Triton X-100 enhanced the increment of fluorescence emission intensity. The increased fluorescence intensity was linearly related to BSA concentration in the range of 0.5-12.0 µg/ml, and under the optimal conditions, the obtained LOD was 0.2 µg/ml, reporting a little interference among amino acids, sugars and most of the metal ions [76].

2,4-dihydroxyl-3-iodo salicylaldehyde azine (DISA) is another turn-on synthesized fluorescent probe which has been used in a novel fluorescence-based method for the detection of HSA and BSA in aqueous solutions. The synthesis of DISA starts with the 3-iodation of 2,4-dihydroxylbenzaldehyde, in which K_2CO_3 and I_2 were added to a solution of 2,4-dihydroxylbenzaldehyde in CH_3CNAs (Figure 5F). Then, the obtained product is allowed to react with hydrazine hydrate in ethanol at room temperature to produce DISA. At a wavelength of 529 nm, a fluorescence turn-on effect after the addition of DISA to the solutions of HSA/BSA can be observed with a significant Stokes shift of ~129 nm which is based on the hydrophobic binding mode of the synthesized dye to albumins. Under the optimal condition, the linear ranges of fluorescence intensity for BSA was 0.1–30 g/ml and the LOD was 50 ng/ml [77].

Enoxacin (ENX) is an antibacterial fluoroquinolone antibiotics drug containing carboxyl and carbonyl active functional groups (Figure 5G). Due to a high-energy transfer from ligand to

the metal ions, ENX is recognized as a suitable compound forming complexes with high stability. Accordingly, ENX-aluminium (Al^{3+}) is reported as another fluorescence probe for the determination of BSA concentrations. This spectrofluorimetric method is claimed to be simple, sensitive, and selective. The detection is based on the fluorescence intensity enhancement of ENX upon the addition of Al^{3+} ions to the solution of ENX. The proposed reaction involves the charge transfer to form a binary complex of ENX-Al^{3+}. In Briton-Robinson buffer (pH=5.8) and in the presence of BSA, the fluorescence intensity of the ENX-Al^{3+} complex was further increased. Also, it was found that under the optimum condition, the enhanced fluorescence intensity was linear for the BSA concentrations in the range of 0.13 to 10.0 ng/ml. The LOD was calculated to be 0.03 ng/ml. The suggested fluorescence-based method provided a simple, less expensive, highly sensitive and wide linear range for determination of BSA compared to other described techniques [78].

3.2.2. Fluorescence resonance energy transfer (FRET)

FRET is recently accepted as a more sensitive and powerful spectroscopic technique which has been widely used in structural biology and analytical chemistry [9, 14]. Generally, the FRET is a distance-dependent phenomenon and the nonradiative energy of one molecule in an excited state as donor or fluorophore transfers to another molecule as acceptor without the emission of a photon. The efficiency of FRET fluorescence energy transfer mainly depends on the overlap region between the emission spectra and absorption spectra of donor and acceptor, respectively, which is higher than 30% and the distance below 10 nm. The developed methods based on FRET for BSA detection has been recognized to be sensitive, adaptable, and fast responding [79]. As proof of concept, a convenient, rapid and susceptible FRET method has been reported for the determination of BSA [80]. In this investigation,

Rhodamine-6G (R6G) and gold nanoparticles (AuNPs) were used as donor and acceptor molecules, respectively. The developed method is advantageous because the employed AuNPs have high quenching efficiency, so the absorption spectra changes from 521 to 635 nm when AuNPs are aggregated. Besides, when R6G was electrostatically adsorbed on the surface of the citrate-stabilized AuNPs, the fluorescence intensity was eliminated. After the addition of BSA, the fluorescence intensity of the R6G recovered as BSA induced aggregation of the AuNPs and the adsorbed R6G was released to the solution (Figure 6A). The intensity recovery showed a linear relationship with the concentration of BSA in the range of 0.8×10^{-11} M to 5.6×10^{-11} M. The LOD for BSA was reported to be 4.58×10^{-11} M. This FRET-based method presented rapid analysis for BSA determination with high selectivity in serum and urine samples.

The efficiency of FRET can be improved in the presence of cetyltrimethylammonium bromide micelles, as it can considerably decrease the distance between the donor and acceptor [81]. Such that, using neutral red (NR) and Cadmium telluride quantum dots (CdTe QDs) as acceptor and donor molecules, respectively, FRET-based molecular sensor is reported to effectively recognize BSA protein in micelles (Figure 6B). Results showed that the addition of the albumin quickly quench the fluorescence emission of CdTe QDs-NR due to the formation of CdTe-albumin complexes. In the presence of BSA, NR dyes affinity to CdTe QDs is weak and thus, repels from the surface of CdTe QDs. With increasing the concentration of albumin, however, the quenching of fluorescence intensity of the CdTe QDs sensor was enhanced which was proportional to the linear range from 0.4×10^{-3} to 11.00×10^{-3} g/l of albumin. The results of these experiments revealed a good sensitivity for BSA detection with a LOD of 0.13 g/l.

4. Nanomaterial-based sensors

4.1. Magnetic nanoparticles (MNPs)

MNPs have recently attracted a growing interest in biological applications due to their excellent biocompatibility. Notably, they can only be separated and purified from different samples using a magnetic field. Therefore, additional complicated steps such as centrifugation are not required. The direct use of MNPs for the detection of BSA has not been reported so far in the literature, and the available research is mostly related to their employment in combination with other nanomaterials for the fabrication and development of new tools for the sensing of trace amounts of BSA. For example, the fabrication of a surface imprinting biosensor is reported based on molecularly imprinted polymers (MIPs) method [82] and MNPs were coated with chitosan (CS) and assembled on the modified multi-walled carbon nanotubes (MWCNTs) on a carbon electrode (CE) (MIPs/MNPs/CS-MWCNTs/CE). MNPs along with CS and MWCNTs acted as signal amplifier, enhancing the sensory function of the biosensor. In a recently published paper by Guoning, Pengqi, Yan, Lu, Hua, Yunzhe, Wanghui, Chun and Qiang [83], a biomimetic ELISA was developed in which Fe_3O_4 NPs was used as a magnetic core. Fe_3O_4 was also successfully employed in the synthesis of surface-imprinted magnetic polymer which was based on atomic transfer radical polymerization (ATRP) method [84].

4.2. Nanomaterials based on Gold

4.2.1. AuNPs

Acceptable biocompatibility, high surface area, good conductivity, electrical and catalytic activities of AuNPs make them a suitable material for different applications [85, 86]. Recently, the operation of a simple and reproducible method is reported to obtain surface-enhanced Raman scattering (SERS) substrate using the efficiently guiding localized surface plasmon resonance (LSPR) field of the trapped AuNPs in the nanochannels of a blu-ray digital versatile disc (BRDVD) [87]. LSPR is known as an optical phenomenon created by a light wave trapped within conductive NPs smaller than the light wavelength. The phenomenon is the result of the interactions between the incident light and surface electrons in a conduction band [88]. In this report, the trapped AuNPs generated guided mode resonance (GMR) field in the BRDVD channel. The suggested SERS substrate produced reasonably stable signal intensity over 45 days. Raman signal intensities of three clinically essential biomolecules, namely albumin, creatinine, and urine, have been measured and quantified reliably with the designed substrate. 0.1 μg/ml, 0.2 μg/ml and 0.6 μg/ml were the minimum concentrations of albumin, creatinine, and urea, respectively measured by Raman spectrometer [87].

AuNPs can also be employed for the fabrication of a modified gold electrode (GE) coated with two dimensional (2D) silica network/citrate-capped AuNPs-poly diallyl dimethyl ammonium chloride (GE–2DSN-CAuNPs-PDDA) which has been successfully used for the ultra-trace determination of BSA protein [89]. Due to the presence of insulated silica network, PDDA was used as the main component of the sensor for electrode modification which provided high impedance and increased the electrode surface area. Further, electrochemical impedance spectroscopy (EIS) was used to evaluate the analytical properties of the developed sensor. In this work, 2D silica network via twice *In situ* hydrolysis of 3-mercaptopropyl-tri-ethoxy silane was covalently attached on the surface of the GE. CAuNPs

were then adsorbed chemically in the silica cage. PDDA was then linked to CAuNPs through the electrostatic interaction of the positively charged polymer, and the CAuNPs stabilized with negative charges. The measured BSA detection limit was reported to be 8.4×10^{-13} mol/l, and the fabricated sensor showed a linear concentration in the range of 9.9×10^{-12} - 1.6×10^{-10} mol/l of protein. Additionally, it produced acceptable results with selectivity and excellent stability in some tested samples for BSA determination (Figure 7).

Equally, AuNPs has been found as useful materials in the preparation of a 3D molecularly imprinted electrochemical sensor based on AuNPs@Ti based metal-organic frameworks with application in ultra-trace BSA detection [90]. The fluorescence turn-off properties of AuNPs make them a suitable nanomaterial in the development of biosensors based on the FRET phenomenon. In these types of biosensing devices, AuNPs act as acceptor molecules and quench the fluorescence emission intensity of the donor molecules [80].

4.2.2. Gold nanorods (Au NRs)

Due to the excellent radiative and nonradiative properties, Au NRs as one dimensional (1D) anisotropic nanomaterials have developed for a wide range of application in different areas such as biomedicine and biology. Au NRs are usually chosen as the nanocarrier for loading different objects to fabricate multifunctional nanoprobes with a high specific surface area [85]. In this respect, the development of a simple label-free fluorescent biosensor based on Au NRs for the assay of BSA and calf thymus DNA (ctDNA) was reported [79]. The coated Au NRs by mesoporous silica ($Au@SiO_2$) were then loaded with acridine orange (AO) using the one-pot synthesis method and the detection of BSA was based on the quenching of fluorescence intensity signal. Under the optimal conditions, the values of the fluorescence quenching intensity obtained from the biosensor were proportional to various concentrations

of BSA (0.75–33.86 mol/l), and the obtained LOD was 0.25 mol/l. A good selectivity for both BSA and ctDNA samples was proposed for this method which can be used in the analysis of the analytes in real samples. The preparation strategy of Au NRs@SiO_2-AO complex was suggested as a novel way to develop fluorescent-based sensors.

4.3. Nanomaterials based on Zinc oxide (ZnO)

4.3.1. Zinc oxide microwires

Due to recent technological achievements, the application of ZnO nanomaterials for the design of biosensors is of considerable interest [91], as they are biologically compatible, and non-toxic with a high chemical stability [92]. In this view, fabrication of a customized electronic platform is demonstrated for biosensing, by integrating a single functionalized microwire between gold microelectrodes as a sensing element, including a custom microelectronic chip for signal readout [93]. The platform was validated as a proof of concept for the real-time detection of BSA binding onto an NH_2-functionalized zinc oxide (ZnO-NH_2) microwire. The ZnO-NH_2 microwire was deposited with dielectrophoresis (DEP) technique between two gold electrodes. A quasi-digital impedance converter (QDIC) was designed to read ZnO microwire impedance continuously and immediately and to transmit data to a laptop. Further, for a better reduction of noise and the functionality of the device, a QDIC, microelectrodes, a DEP generator, and data analysis were incorporated in a stacked-card PCB configuration. The proposed system in this study was capable of differentiating between different BSA concentrations and provided real-time information on the binding process (Figure 8).

4.3.2. ZnO nanospheres

An electrical detection method based on solution-processed zinc oxide nanosphere for ultra-low BSA detection has been demonstrated. The developed device worked with different BSA concentrations based on the variation in the conductance of the ZnO nanosphere displaying the sensitivity of 0.126 nA/pM, LOD of 10 pM and the fast response time about 5 s. Authors claimed that they achieved the highest sensitive detection sensor for BSA so far. The basis of the sensing mechanism was charge transfer between ZnO and BSA [94].

4.3.3. Al_2O_3/ZnO nanolaminates

As an extra platform for BSA detection, Al_2O_3/ZnO nanolaminates have been assessed for possible use in optical immunosensor design [95]. To this, optical response of the prepared nanolaminates that was pre-modified with an N-(3-aminopropyl) triethoxysilane (APTES) layer during the formation of BSA monolayer on the surface of Al_2O_3/ZnO sensor was studied using the total internal reflection ellipsometry (TIRE) technique. Results demonstrated a significant contribution of multiple reflections from the interfaces between ZnO and Al_2O_3 to the improvement of the optical response in the total internal reflection configuration. Furthermore, Al_2O_3/ZnO nanolaminates with a total thickness of 200 nm based on four alternating Al_2O_3 and ZnO layers with a thickness of 50 nm showed a higher sensitivity than nanolaminates with two 100 nm oxide layers.

4.4. Nanomaterials based on silver

4.4.1. Silver nanoparticles (AgNPs)

Recently, a wide range of analytical applications has been reported for AgNPs due to their unique optical properties in the LSPR. AgNPs of various sizes and shapes display different colors depending on their LSPR absorption in the visible spectral range. Therefore, tremendous research is focused on the preparation of AgNPs of various shapes and sizes, such as nanotubes, nanowires, nanorods, nanodiscs/nanoplates, nanoprisms, triangular silver nanoplates (TAgNPs), and so on [96]. In an investigation by Pan, Tao, Mao, Zhu and Liang [97], a new method for preparing a series of functionalized silver sulfide nanoparticles (Ag_2S NPs) with different amino polycarboxylic acids is proposed. That, based on the resonance light scattering (RLS) spectra intensities enhanced by BSA-induced Ag_2S NPs aggregation, a sensitive RLS method for the BSA detection was realized at nanogram detection levels. The LOD for BSA was 8.6 and 112.6 ng m/l, which was dependant on the used capping agents. Also, LOD was affected by the stability constant (log K_{MY}) for the complexes of silver and aminopolycarboxyl agents.

In addition, quantitative analysis of SERS studies shows that the SERS intensity of BSA adsorbed on the AgNPs substrate deposited at 300 °C is higher than that of BSA adsorbed on the active substrates of SERS at any other substrate temperature (Ts) [98]. In one experiment, AgNPs thin films were produced on glass substrates by pulsed laser deposition at 0.1 mbar pressure, and different applied Ts in a controlled Argon atmosphere and the effect of Ts on electrical conductance, surface plasmon resonance (SPR), and SERS activity of AgNPs thin films is described. Results indicated the film deposited at room temperature has an SPR peak of 460 nm, and its wavelength increases first until Ts reaches 300 ° C and then decreases with further increase in Ts.

4.4.2. TAgNPs

An extra method for BSA quantification can be envisaged using TAgNPs. In this way, interactions of TAgNPs and BSA in the Britton–Robison buffer solution (BR), is reported as a fast, simple, and ultra-sensitive spectrophotometric techniqueZhang, Ma, Kuang, Cheng, Long and Xiao [99] for BSA detection. In the reported work, in BR buffer solution (pH = 2.56), the maximum absorption wavelength (λ_{max}) of TAgNPs showed a red shift in the presence of BSA molecules and the color solution changed from blue to light blue. It was demonstrated that at pH 2.56, hydrogen bonds (H-bonds), van der Waals forces, electrostatic forces, and hydrophobic effects are the main interactions stabilizing BSA molecules on the surface of TAgNPs, causing the TAgNPs aggregation. Further, the change of λ_{max} corresponding to LSPR obtained from UV–vis spectrophotometry was measured for BSA determination. Results showed that the shift value in the maximum absorption wavelength ($\Delta\lambda$, the difference in the λ_{max} of the TAgNPs/BR in the presence and absence of BSA) was proportional to the BSA concentration in the range of 1.0-100.0 ng /ml. The LOD for BSA was found to be 0.5 ng/ml.

4.4.3. Silver nanostructures (AgNSs)

AgNSs has also been examined in the detection of BSA by Devi, Berchmans and Mandal [100]. They demonstrated a new protein test using the voltammetric method in the presence of AgNSs, which were electrochemically formed on gold substrates modified with a monolayer of self-assembled thioctic acid. The fabricated AgNSs possessed voltammetric response characteristic of Ag, and under physiological pH, they displayed near Nernstian response. In comparison to the conventional protein assays, the authors claimed that the modified electrochemical method shows some advantages including the wide linear range for

BSA concentration (10^4–10^{11} g/ml) and low level of LOD (50 pg/ml). Additionally, long term stability and high sensitivity were reported for the developed electrode.

4.5. GO-based nanomaterials

In recent decades, GO has been gained much-increasing interest since the first report in 2004, as it is a 2D unique graphitic carbon nanomaterial with only one atom thickness. It can be directly transformed into monolayer sheets and is capable of preparing highly stable dispersions in water. These properties are primarily attributed to their oxygen containing functional groups, such as alcohols, carboxylic acid, and epoxides. GO shows various specific characteristics such as electron confinement effects, extremely high theoretical surface area, electromechanical modulation, good optical transparency, excellent thermal/chemical stability and high mechanical flexibility [101]. In the context of protein detection, the interaction of GO, 10-hydroxy camptothecin (HCPT) as a medicinal anticancer drug, and BSA was explored for the development of a method for serum albumin analysis [102]. It was shown that HCPT binding and loading on GO surface was due to π-π stacking interaction, and in the presence of GO, the delivery of HCPT to BSA was improved (Figure 9). Thus, GO could facilitate the binding interaction between HCPT and BSA. Moreover, GO was found to enhance HCPT's fluorescence response to BSA and thus, a low-cost biosensing platform for fluorescence turn-on BSA detection based on GO was developed. The structure and electronic properties of GO were attributed to the satisfactory analytical performance of this biosensor for BSA discrimination and further quantification.

4.6. Carbon nanotubes

In the last decade, considerable effort has been made to use MWCNTs as new biosensing nanomaterials. MWCNTs-based sensors with a high specific surface area are expected to show high sensitivity and rapid response [103]. MWCNTs have been extensively used in the construction of sensing devices for selective and sensitive BSA detection and quantification. In this regard, numerous MIPs have been prepared and reported in the literature for the recognition of bovine albumin. Chen, Zhang, Luo and Yao [82] used MWCNTs for the fabrication of a different sensing device composed of surface-imprinted chitosan-coated MNPs modified MWCNTs for the detection of BSA. In another research reported by Zhang, Huang, Yu and Chen [104], the surface of MWCNTs was used for the development of a new protein molecularly imprinted membranes (MIMs) for BSA recognition. For the ultra-trace detection of BSA, the MWCNTs bearing vinyl exposed groups on ceramic electrode were modified to fabricate MIPs with high substrate-selective properties [105]. Likewise, in an investigation reported by Zhang, Huang, Yu and Chen [104], the surface of MWCNTs was used for the preparation of MIMs, and the adsorption characteristics of the prepared MIMs toward BSA were evaluated.

4.7. QDs

Organic dyes are the common chemicals used for the sensing of different molecules and cell imaging based on fluorescence methods. In recent years, QDs as monodispersed colloidal semiconductor nanocrystals have attracted significant attention and have also attracted considerable research efforts over conventional fluorophores due to their excellent optical properties such as high quantum yields, strong resistance to photobleaching, broad absorption spectra, size-tunable, symmetric and narrow emission bands (30-50 nm), high photostability, and high photoluminescence efficiency [106].

For detection of BSA using CdTe QDs and neutral red, Ge, Lu, Yan, Yu, Yu and Sun [81] developed a FRET-based sensor. In this investigation, using CdTe QDs and NR as energy donors and acceptors, respectively, BSA in micelles was effectively sensed by a FRET-based molecular sensor. Results proposed a new technique for BSA determination, which was based on the electrochemiluminescence (ECL) of BSA with CdTe QDs films. Firstly, the substrates were dipped into the toluene solution of 3-aminopropyltrimethoxysilane (APS) to obtain an APS layer. Then, stable water-soluble QDs with intensive anodic ECL emission were obtained using thioglycolic acid (TGA) to cap CdTe colloidal solutions on an electrode of indium tin oxide (ITO). The modified ITO glass with CdTe QDs was prepared by the layer-by-layer (LbL) self-assembly procedure (Figure 10A). The ECL intensity was reported to be linear with BSA content in the concentration range of 1.0×10^{-9}–1.0×10^{-6} g/ml and 1.0×10^{-6}-1.0×10^{-5} g/ml, and the calculated LOD was 5.48×10^{-10} g/ml. A good reproducibility for ECL analysis was accomplished using this sensitive and straightforward method [107]. Also, for the quantitative determination of BSA, a novel method is presented by Yu, Lai, Zheng, Wu, Long and Liang [108]. In this study, a new type of functionalized CdTe/CdS QDs was synthesized for quantitative and selective sensing and determining of BSA. Fluorescence intensity with maximum excitation and emission wavelengths were detected at 336 and 524 nm, respectively at pH 6.83. Under optimal conditions, the concentration of BSA were in the range of 0-1.2×10^{-6} mol dm^{-3} and the obtained fluorescence intensity was reported to be linear, with LOD of 5.4×10^{-8} mol dm^{-3}. In addition to its reliable fluorescence signaling and intrinsic sensitivity, other benefits of this method included its simplicity, highly resistant to chemical and metabolic degradation, rapidity, significant Stokes shift, and good water-solubility. Similarly, silica nanospheres surface surrounded CdTe QDs were prepared in a new epitope-based molecular imprinting polymers (EMIPs) for the recognition of BSA [109].

In this attempt, the CdTe QDs were directly modified by the sol-gel reaction with $NH_3.H_2O$ as a catalyst to accelerate the reaction with a silica shell, and the synthetic peptide was used as a template molecule from the C-terminus of BSA. Compared to MIPs coating CdTe QDs using BSA as the template, the direct fluorescence quantification of BSA for the MIPs coating CdTe QDs nanospheres using epitope as the template was affordable.

Further, InGaP/ZnS core-shell biocompatible functionalized QDs were bioconjugated with polyclonal anti-BSA antibody and used as fluorescent probes for BSA detection. The characterized absorption and emission spectra blue shifting around 40 and 30 nm, respectively showed strong bioconjugation reactions. The conjugation was performed using 1-ethyl-3-(3-dimethylaminopropyl) carbodiimide (EDC) as a crosslinker to create a peptide bond between the amide group of QDs and the carboxyl group of anti-BSA (Figure 10B). SPR spectrometry exploited to study the affinity of QDs-anti-BSA probes for BSA detection, corroborating that the developed probe is capable of the photoluminescence quenching of BSA [110].

5. Other related works of interest

For the quantification of BSA in milk products, an automated biosensor immunoassay using SPR has been described [111]. The LOD of the suggested method was 0.02 mg/g in milk and at least for 400 cycles, a single flow cell was stable. This technique was used to estimate the BSA content of bovine milk, colostrum, whey protein fractions and formulae for infants. SPR sensitivity enabled the reduction of non-specific interactions and high sample dilution. A label-free, real-time quantitation of BSA is proposed with the development of automated biosensor immunoassay in bovine milk products and pediatric formulae, which is sensitive, precise, rapid, and accurate, providing data comparable to the high-performance liquid

chromatography (HPLC). For highly sensitive quantitation of BSA, its iron-binding properties were considered in the report by Kukkar, Sharma, Kumar, Kim and Deep [112], which describes the application of a new molybdenum disulfide (MoS_2) based on an electrochemical platform. Authors modified the screen-printed gold electrodes with MoS_2 nanoflakes and subsequently bioconjugated it with anti-BSA antibodies. The constructed bioelectrode exhibited a linear response with the LOD of 0.006 ng/ml. The method showed a significant improvement in the signal during the electrochemical sensation of a protein. The applicability of the developed strategy in this research can also be extended to the sensing of several other protein molecules with iron-binding properties, such as HSA, transferrin, ferritin, and lactoferrin. The attachment of antibody on the surface of MoS_2 nanoflakes was claimed to be simple, which achieved by hydrophobic interactions. It is reported that the direct protein oxidation peaks could be observed by H-terminated boron-doped diamond (BDD) electrodes. Further, BDD enabled hydrogen production by reduction treatment. The pH dependence of BSA oxidation suggested that the oxidation involved at least three redox-active amino acid residues (Trp, Cys, and Tyr). A linear concentration range of 5 to 3000 mg/dl with a lower LOD of 5 mg/dl was determined for BSA. A good reproducibility was also accomplished, suggesting that BDD electrodes can be used for direct electrochemical detection with a high sensitivity, stability, and simplicity [113]. Moreover, near-infrared diffuse reflectance spectroscopy (NIRDRS) is considered as a powerful method for analyzing samples components with complex matrices. However, the use of this method for microanalysis still presents certain obstacles to be overcome, such as low sensitivity and spectral overlapping. Using NIRDRS with sample spots and chemometric techniques, a method for the fast determination of BSA in micro-volume samples was studied. For spectral measurements, only 10 μl of the spotted sample on a filter paper substrate was used and

suggested that the method had the potential to quickly detect proteins in low volume solutions [114]. Equally, monitoring of BSA using piezoelectric quartz crystal impedance (QCI) method with the precipitation of BSA in the presence of Cu^{2+}ions was reported [115]. For BSA determination, the linear range of 4×10^{-3} to 4×10^{-1} g/l with the LOD of 1.9×10^{-4} g/l was achieved. This method is simple since no additional reagent is required. Also, it is suitable for determining other proteins and can be used to study the dynamics process.

The conjugated polydiacetylenes (PDAs) polymers with the unique intrinsic ability to respond to various stimuli undergo the transition of blue to red. Some PDA-based systems have been designed to detect bacteria, enzymes, viruses, surfactants, solvents and so on using colorimetric changes. These chromic properties of PDA makes it a suitable material for application in sensor systems with several advantages, such as fast and straightforward detection, easy color change recognition by the naked eye and label-free detection. In an attempt, nano-aggregates formed by a mixture of two polymers (PDA and triblock copolymer L64) was used to overcome the limitations of PDA vesicles and used for detection of BSA. This work describes the properties of the synthesized polydiacetylene-triblock copolymer (L64) nanosensors, for easy detection of BSA. The function of nanosensor composition, polydiacetylene chemical structures, BSA conformation, and hydrophobic domain availability was considered to evaluate the sensor efficiency. The developed nanosensors were sensitive to the average BSA concentration in milk and dairy products. Moreover, it has been discriminated by naked eye blue to red transition the native and denatured BSA. Discriminating between free/bound and native/denatured protein as the main property of the constructed PDA-L64 nanosensor has the potential to be used as an inexpensive sensor for rapid BSA detection [116].

6. Conclusions

Bovine albumin is the main protein in products obtained from cows such as milk and meat, and its detection and quantification is of great importance due to increasing the consumption of such foods in recent decades. Additionally, BSA is a vital protein widely used in different biomedical assays, and thus, it has been attempted to sense and quantify this biomolecule using different methods. Because of considerable accuracy, high sensitivity, efficiency, and high-speed measurement, modern nanotechnology-based detection methods have been successfully applied as superior alternatives to the conventional biosensing methods in recent years. Due to their unique features, different types of metallic or non-metallic NPs including AuNPs, MNPs, QDs, and so on have attracted particular attention. The combination of different nanomaterials with sensitive spectroscopic techniques such as fluorescence and SPR can provide the ultra-amounts detection of albumin. The fluorescence turn-on properties of some molecules make them a suitable candidate in the robust recognition of BSA. Though the recent two decades have witnessed a considerable achievement in BSA detection methodologies, nonetheless, none of the developed methods has paved the way to the industrial/market uses. Thus, it seems that the current knowledge and the reported methods and the constructed devices on albumin recognition is not adequate and the improvement and development of novel methods for real uses in different fields is indispensable.

Conflict of interest

The authors declare no conflicts of interest.

Acknowledgments

The authors appreciate the support of this review by the Nutrition Research Center, Student Research Committee, Infectious and Tropical Diseases Research Center, Tabriz University of Medical Sciences, Tabriz, Iran and the Institute of Animal Reproduction and Food Research, Olsztyn, Poland.

References

[1] M. Vaudel, A. Sickmann, L. Martens, Peptide and protein quantification: a map of the minefield, Proteomics 10(4) (2010) 650-670.

[2] J.E. Noble, M.J. Bailey, Quantitation of protein, Methods in enzymology, Elsevier2009, pp. 73-95.

[3] W. Tao, W. Li, Y. Jiang, Protein molecular basic, The People's Education Press: p 256 (1981).

[4] A. Jahanban-Esfahlan, V. Panahi-Azar, Interaction of glutathione with bovine serum albumin: Spectroscopy and molecular docking, Food Chemistry 202 (2016) 426-431.

[5] L. Roufegarinejad, A. Jahanban-Esfahlan, S. Sajed-Amin, V. Panahi-Azar, M. Tabibiazar, Molecular interactions of thymol with bovine serum albumin: Spectroscopic and molecular docking studies, Journal of Molecular Recognition (2018) Doi: 10.1002/jmr.2704.

[6] A. Jahanban-Esfahlan, V. Panahi-Azar, S. Sajedi, Spectroscopic and molecular docking studies on the interaction between N-acetyl cysteine and bovine serum albumin, Biopolymers 103 (2015) 638-645.

[7] J.K. Maurya, M.U.H. Mir, N. Maurya, N. Dohare, A. Ali, R. Patel, A spectroscopic and molecular dynamic approach on the interaction between ionic liquid type gemini surfactant and human serum albumin, Journal of Biomolecular Structure and Dynamics 34(10) (2016) 2130-2145.

[8] N. Maurya, J.K. Maurya, U.K. Singh, R. Dohare, M. Zafaryab, M. Moshahid Alam Rizvi, M. Kumari, R. Patel, In vitro cytotoxicity and interaction of noscapine with human serum albumin: Effect on structure and esterase activity of HSA, Molecular Pharmaceutics 16(3) (2019) 952-966.

[9] A. Jahanban-Esfahlan, S. Davaran, A.A. Moosavi-Movahedi, S. Dastmalchi, Investigating the interaction of juglone (5-hydroxy-1, 4-naphthoquinone) with serum albumins using spectroscopic and in silico methods, Journal of the Iranian Chemical Society 7(14) (2017) 1527-1540.

[10] M. Kumari, U.K. Singh, P. Singh, R. Patel, Effect of N-butyl-N-methyl-Morpholinium bromide ionic liquid on the conformation stability of human serum albumin, ChemistrySelect 2(3) (2017) 1241-1249.

[11] R. Patel, N. Maurya, M.U.D. Parray, N. Farooq, A. Siddique, K.L. Verma, N. Dohare, Esterase activity and conformational changes of bovine serum albumin toward interaction with mephedrone: Spectroscopic and computational studies, Journal of Molecular Recognition 31(11) (2018) e2734.

[12] R. Patel, M.U.H. Mir, J.K. Maurya, U.K. Singh, N. Maurya, M.u.d. Parray, A.B. Khan, A. Ali, Spectroscopic and molecular modelling analysis of the interaction between ethane-1, 2-diyl bis (N, N-dimethyl-N-hexadecylammoniumacetoxy) dichloride and bovine serum albumin, Luminescence 30(8) (2015) 1233-1241.

[13] A. Jahanban-Esfahlan, S. Dastmalchi, S. Davaran, A simple improved desolvation method for the rapid preparation of albumin nanoparticles, International Journal of Biological Macromolecules 91 (2016) 703-709.

[14] L. Roufegarinejad, R. Amarowicz, A. Jahanban-Esfahlan, Characterizing the interaction between pyrogallol and human serum albumin by spectroscopic and molecular docking methods, Journal of Biomolecular Structure and Dynamics (just-accepted) (2018) 1-36.

[15] H. Andishmand, L. Roufegari Nejad, M. Tabibiazar, Nanostructure characterization of bovine serum albumin-resveratrol complex, Journal of Research and Innovation in Food Science and Technology 6(3) (2017) 291-300.

[16] M. Tabibiazar, S. Davaran, M. Hashemi, A. Homayonirad, F. Rasoulzadeh, H. Hamishehkar, M.A. Mohammadifar, Design and fabrication of a food-grade albumin-stabilized nanoemulsion, Food Hydrocolloids 44 (2015) 220-228.

[17] T.T. Lee, E.S. Yeung, High-sensitivity laser-induced fluorescence detection of native proteins in capillary electrophoresis, Journal of Chromatography A 595(1-2) (1992) 319-325.

[18] G.L. Long, J.D. Winefordner, Limit of detection. A closer look at the IUPAC definition, Analytical chemistry 55(7) (1983) 712A-724A.

[19] P.G. Pande, R.V. Nellore, H.R. Bhagat, Optimization and validation of analytical conditions for bovine serum albumin using capillary electrophoresis, Analytical biochemistry 204(1) (1992) 103-106.

[20] W. Jin, Q. Weng, J. Wu, Determination of bovine serum albumin by capillary zone electrophoresis with end-column amperometric detection at the carbon fiber microdisk array electrode, Analytica Chimica Acta 342 (1997) 67-74.

[21] U. Nguyen, N. Squaglia, A. Boge, P.A. Fung, The Simple Western™: a gel-free, blot-free, hands-free Western blotting reinvention, Nature Methods 8(11) (2011) v-vi.

[22] J.W. Loughney, C. Lancaster, S. Ha, R.R. Rustandi, Residual bovine serum albumin (BSA) quantitation in vaccines using automated Capillary Western technology, Analytical biochemistry 461 (2014) 49-56.

[23] J.R. Lakowicz, Principles of fluorescence spectroscopy, third ed., Springer science+Business Media, New York, 2006.

[24] B. Valeur, Molecular Fluorescence: Principles and Applications, Wiley, New York, 2001.

[25] K. Kaibara, T. Okazaki, H.B. Bohidar, P.L. Dubin, pH-Induced coacervation in complexes of bovine serum albumin and cationic polyelectrolytes, Biomacromolecules 1 (2000) 100-107.

[26] A. Papadopoulou, R.J. Green, R.A. Frazier, Interaction of flavonoids with bovine serum albumin: A fluorescence quenching study, Journal of Agricultural and Food Chemistry 53 (2005) 158-163.

[27] K.Y. Pu, B. Liu, Fluorescence turn-on responses of anionic and cationic conjugated polymers toward proteins: Effect of electrostatic and hydrophobic interactions, The Journal of Physical Chemistry B 114 (2010) 3077-3084.

[28] T. Zhou, M.Q. Ao, G.Y. Xu, T. Liu, J. Zhang, Interactions of bovine serum albumin with cationic imidazolium and quaternary ammonium gemini surfactants: Effects of surfactant architecture, Journal of Colloid and Interface Science 389 (2013) 175-181.

[29] L.Y. Wang, H.H. Li, G.P. Fang, J.A. Zhou, D.R. Cao, Fluorescence enhancement of water-soluble porphyrin-containing conjugated polymer induced by DNA and cellular imaging in living cells, Sensors and Actuators B: Chemical 196 (2014) 653-662.

[30] D. Wang, J. Qian, W. Qin, A. Qin, B.Z. Tang, S. He, Biocompatible and photostable AIE dots with red emission for in vivo two-photon bioimaging, Scientific Reports 4 (2014) 4279.

[31] H. Tong, Y.N. Hong, Y.Q. Dong, M. Häußler, J.W.Y. Lam, Z. Li, Z.F. Guo, Z.H. Guo, B.Z. Tang, Fluorescent "light-up" bioprobes based on tetraphenylethylene derivatives with aggregation-induced emission characteristics, Chemical Communications 0(35) (2006) 3705-3707.

[32] M. Wang, D.Q. Zhang, G.X. Zhang, D.B. Zhu, The convenient fluorescence turn-on detection of heparin with a silole derivative featuring an ammonium group, Chemical Communications 0 (2008) 4469-4471.

[33] M. Wang, G.X. Zhang, D.Q. Zhang, D.B. Zhu, B.Z. Tang, Fluorescent bio/chemosensors based on silole and tetraphenylethene luminogens with aggregation-induced emission feature, Journal of Materials Chemistry 20(1858-1867) (2010).

[34] Z.G. Song, Y.N. Hong, R.T.K. Kwok, J.W.Y. Lam, B. Liu, B.Z. Tang, A dual-mode fluorescence "turn-on" biosensor based on an aggregation-induced emission luminogen, Journal of Materials Chemistry B 2 (2014) 1717-1723.

[35] X.G. Gu, G.X. Zhang, D.Q. Zhang, A new ratiometric fluorescence detection of heparin based on the combination of the aggregation-induced fluorescence quenching and enhancement phenomena, Analyst 137 (2012) 365-369.

[36] R.T.K. Kwok, J.L. Geng, J.W.Y. Lam, E.G. Zhao, G. Wang, R.Y. Zhan, B. Liu, B.Z. Tang, Water-soluble bioprobes with aggregation-induced emission characteristics for light-up sensing of heparin, Journal of Materials Chemistry B 2 (2014) 4134-4141.

[37] H. Zhang, Y. Qu, Y.T. Gao, J.L. Hua, J. Li, B. Li, A red fluorescent 'turn-on' chemosensor for Hg^{2+} based on triphenylamine–triazines derivatives with aggregation-induced emission characteristics, Tetrahedron Letters 54 (2013) 909-912.

[38] Y.Y. Yuan, R.T.K. Kwok, B.Z. Tang, B. Liu, Targeted theranostic platinum(IV) prodrug with a built-in aggregation-induced emission light-up apoptosis sensor for noninvasive early evaluation of its therapeutic responses in situ, Journal of the American Chemical Society 136 (2014) 2546-2554.

[39] Y.Y. Huang, F. Hu, R. Zhao, G.X. Zhang, H. Yang, D.Q. Zhang, Tetraphenylethylene conjugated with a specific peptide as a fluorescence turn-on bioprobe for the highly specific detection and tracing of tumor markers in live cancer cells, Chemistry A European Journal 20 (2014) 158-164.

[40] C.J. Kassl, F.C. Pigge, Anion detection by aggregation-induced enhanced emission (AIEE) of urea-functionalized tetraphenylethylenes, Tetrahedron Letters 55 (2014) 4810-4813.

[41] M.M. Wienk, M. Turbiez, J. Gilot, R.A. Janssen, Narrow-bandgap diketo-pyrrolo-pyrrole polymer solar cells: The effect of processing on the performance, Advanced Materrials 20 (2008) 2556-2560.

[42] T.L. Chen, Y. Zhang, P. Smith, A. Tamayo, Y. Liu, B.W. Ma, Diketopyrrolopyrrole-containing oligothiophene-fullerene triads and their use in organic solar cells, ACS Applied Materials and Interfaces 3 (2011) 2275–2280.

[43] C.H. Yang, E.J. Zhou, S. Miyanishi, K. Hashimoto, K. Tajima, Preparation of active layers in polymer solar cells by aerosol jet printing, ACS Applied Materials and Interfaces 3 (2011) 4053-4058.

[44] C.M. Yu, C. He, Y. Yang, Z.X. Cai, H.W. Luo, W.Q. Li, Q. Peng, G.X. Zhang, Z.T. Liu, D.Q. Zhang, New conjugated molecules with two and three dithienyldiketopyrrolopyrrole (DPP) moieties substituted at meta positions of benzene toward p- and n-type organic photovoltaic materials, Chemistry An Asian Journal 9 (2014) 1570-1578.

[45] Y. Zhu, A.R. Rabindranath, T. Beyerlein, B. Tieke, Highly luminescent 1,4-diketo-3,6-diphenylpyrrolo[3,4-c]pyrrole- (DPP-) based conjugated polymers prepared upon Suzuki coupling, Macromolecules 40 (2007) 6981-6989.

[46] Z.Y. Chen, M.J. Lee, R.S. Ashraf, Y. Gu, S. Albert-Seifried, M.M. Nielsen, B. Schroeder, T.D. Anthopoulos, M. Heeney, I. McCulloch, H. Sirringhaus, High-performance ambipolar diketopyrrolopyrrole-thieno[3,2-b]thiophene copolymer field-effect transistors with balanced hole and electron mobilities, Advanced Materials 24 (2012) 647-652.

[47] I. Meager, R.S. Ashraf, S. Rossbauer, H. Bronstein, J.E. Donaghey, J. Marshall, B.C. Schroeder, M. Heeney, T.D. Anthopoulos, I. McCulloch, Alkyl chain extension as a route to novel thieno[3,2-b]thiophene flanked diketopyrrolopyrrole polymers for use in organic solar cells and field effect transistors, Macromolecules 46 (2013) 5961-5967.

[48] H. Sirringhaus, 25th Anniversary Article: Organic field-effect transistors: The path beyond amorphous silicon, Advanced Materials 26 (2014) 1319-1335.

[49] L. Deng, W.T. Wu, H.M. Guo, J.Z. Zhao, S.M. Ji, X. Zhang, X.L. Yuan, C.L. Zhang, Colorimetric and ratiometric fluorescent chemosensor based on diketopyrrolopyrrole for selective detection of thiols: An experimental and theoretical study, The Journal of Organic Chemistry 76 (2011) 9294-9304.

[50] F. He, L.B. Liu, L.D. Li, Water-soluble conjugated polymers for amplified fluorescence detection of template-independent DNA elongation catalyzed by polymerase, Advanced Functional Materials 21 (2011) 3143-3149.

[51] G.J. Zhang, H.Y. Li, S.M. Bi, L.F. Song, Y.X. Lu, L. Zhang, J.J. Yu, L.M. Wang, A new turn-on fluorescent chemosensor based on diketopyrrolopyrrole (DPP) for imaging Zn^{2+} in living cells, Analyst 138 (2013) 6163-6170.

[52] S.M. Lin, S.P. Liu, F.Q. Ye, L. Xu, W.N. Zeng, L.Y. Wang, L. Li, R. Beuerman, D.R. Cao, Sensitive detection of DNA by hyperbranched diketopyrrolopyrrole-based conjugated polyelectrolytes, Sensors and Actuators B: Chemical 182 (2013) 176-183.

[53] M.V.R. Raju, H.C. Lin, A novel diketopyrrolopyrrole (DPP)-based [2] rotaxane for highly selective optical sensing of fluoride, Organic Letters 15 (2013) 1274-1277.

[54] L.Y. Wang, L.L. Yang, D.R. Cao, Detection of HSO_4^- ion based on the hydrolysis of diketopyrrolopyrrole-derived schiff base with chromogenic and fluorogenic dual signals, Journal of Fluorescence 24 (2014) 1347-1355.

[55] L.Y. Wang, L.L. Yang, D.R. Cao, A visual and fluorometric probe for Al(III) and Fe(III) using diketopyrrolopyrrole-based Schiff base, Sensors and Actuators B: Chemical 202 (2014) 949-958.

[56] L.Y. Wang, J.Q. Du, D.R. Cao, A colorimetric and fluorescent probe containing diketopyrrolopyrrole and 1,3-indanedione for cyanide detection based on exciplex signaling mechanism, Sensors and Actuators B: Chemical 198 (2014) 455-461.

[57] B.L. Zhang, H.C. Zhang, X.J. Li, W. Li, P.P. Sun, W.J. Yang, Synthesis, characterization, and large two-photon absorption cross-sections of solid red-emitting 1,4-diketo-3,6-diphenylpyrrolo [3,4-c]pyrrole/3,6-carbazole/terfluorene copolymers, Journal of Polymer Science, Part A: Polymer Chemistry 49 (2011) 3048-3057.

[58] H. Ftouni, F. Bolze, H.D. Rocquigny, J.F. Nicoud, Functionalized two-photon absorbing diketopyrrolopyrrole-based fluorophores for living cells fluorescent microscopy, Bioconjugate Chemistry 24 (2013) 942-950.

[59] Y.T. Gao, Y. Qu, T. Jiang, H. Zhang, N.N. He, B. Li, J.C. Wu, J.L. Hua, Alkyl-triphenylamine end-capped triazines with AIE and large two-photon absorption cross-sections for bioimaging, Journal of Material Chemistry C 2 (2014) 6353-6363.

[60] S.Y. Qu, B. Wang, F.L. Guo, J. Li, W.J. Wu, C. Kong, Y.T. Long, J.L. Hua, New diketo-pyrrolo-pyrrole (DPP) sensitizer containing a furan moiety for efficient and stable dye-sensitized solar cells, Dyes and Pigments 92 (2012) 1384-1393.

[61] J.H. Yum, T.W. Holcombe, Y. Kim, K. Rakstys, T. Moehl, J. Teuscher, J.H. Delcamp, M.K. Nazeeruddin, M. Grätzel, Blue-coloured highly efficient dye-sensitized solar cells by implementing the diketopyrrolopyrrole chromophore, Scienctific Reports 3 (2013) 2446.

[62] Y. Qu, J.L. Hua, H. Tian, Colorimetric and ratiometric red fluorescent chemosensor for fluoride ion based on diketopyrrolopyrrole, Organic Letters 12 (2010) 3320-3323.

[63] T. Okabe, D. Kuzuhara, M. Suzuki, N. Aratani, H. Yamada, Synthesis and electrochemical properties of porphycene–diketopyrrolopyrrole conjugates, Organic Letters 16 (2014) 3508-3511.

[64] H. Patil, A. Gupta, A. Bilic, S.V. Bhosale, S.V. Bhosale, A solution-processable electron acceptor based on diketopyrrolopyrrole and naphthalenediimide motifs for organic solar cells, Tetrahedron Letters 55 (2014) 4430-4432.

[65] S.Y. Qu, C.J. Qin, A. Islam, Y.Z. Wu, W.H. Zhu, J.L. Hua, H. Tian, L.Y. Han, A novel D–A-π-A organic sensitizer containing a diketopyrrolopyrrole unit with a branched alkyl chain for highly efficient and stable dye-sensitized solar cells, Chemical Communications 48 (2012) 6972-6974.

[66] B. Wang, N.N. He, B. Li, S.Y. Jiang, Y. Qu, S.Y. Qu, J.L. Hua, Aggregation-induced emission and large two-photon absorption cross-sections of diketopyrrolopyrrole (DPP) derivatives, Australian Journal of Chemistry 65 (2012) 387-394.

[67] Y. Hang, L. Yang, Y. Qu, J. Hua, A new diketopyrrolopyrrole-based near-infrared (NIR) fluorescent biosensor for BSA detection and AIE-assisted bioimaging, Tetrahedron Letters 55 (2014) 6998-7001.

[68] L. Wang, L. Yang, D. Cao, Probes based on diketopyrrolopyrrole and anthracenone conjugates with aggregation-induced emission characteristics for pH and BSA sensing, Sensors and Actuators B: Chemical 221 (2015) 155-166.

[69] H. Shindy, Fundamentals in the chemistry of cyanine dyes: A review, Dyes and Pigments 145 (2017) 505-513.

[70] H. Li, F. Liu, J. Han, M. Cai, S. Sun, J. Fan, F. Song, X. Peng, Interaction of Cy3 dye with CCG and its application for BSA detection, Journal of Materials Chemistry B 1(5) (2013) 693-697.

[71] X. Xu, J. Huang, J. Li, J. Yan, J. Qin, Z. Li, A graphene oxide-based AIE biosensor with high selectivity toward bovine serum albumin, Chemical Communications 47(45) (2011) 12385-12387.

[72] D.L. Ma, H.Z. He, K.H. Leung, D.S.H. Chan, C.H. Leung, Bioactive luminescent transition-metal complexes for biomedical applications, Angewandte Chemie International Edition 52(30) (2013) 7666-7682.

[73] E. Babu, P.M. Mareeswaran, S. Singaravadivel, J. Bhuvaneswari, S. Rajagopal, A selective, long-lived deep-red emissive ruthenium (II) polypyridine complexes for the detection of BSA, Spectrochimica Acta Part A: Molecular and Biomolecular Spectroscopy 130 (2014) 553-560.

[74] S. Sun, H. Ma, X. Chen, N. Zhang, D. Wu, B. Du, Q. Wei, Fluorimetric determination of proteins using 4-chloro-(2′-hydroxylophenylazo) rhodanine–Ti (IV) complex as a spectral probe, Luminescence 23(5) (2008) 333-337.

[75] Q.-Z. Zhu, J.-G. Xu, X.-Q. Guo, X.-Y. Zheng, W.-Y. Li, Y.-B. Zhao, In-situ photochemical spectrofluorimetric detection of 9, 10-anthraquinone-labeled bovine serum albumin, Spectrochimica Acta Part A: Molecular and Biomolecular Spectroscopy 53(12) (1997) 2195-2200.

[76] S.H. Lee, J.K. Suh, M. Li, Determination of bovine serum albumin by its enhancement effect of Nile Blue fluorescence, Bulletin Korean Chemical Society 24(1) (2003) 45-48.

[77] X.-t. Chen, Y. Xiang, A.-j. Tong, Facile, sensitive and selective fluorescence turn-on detection of HSA/BSA in aqueous solution utilizing 2, 4-dihydroxyl-3-iodo salicylaldehyde azine, Talanta 80(5) (2010) 1952-1958.

[78] Nasiruddin, Kamruzzaman, R. Ahmed, Anwaruzzaman, L. Habib, A. Mannan, Spectrofluorimetric determination of bovine serum albumin using enoxacin-aluminium (III) as a fluorescence probe, American Journal of Biochemistry 8(5) (2018) 100-105.

[79] W. Zhu, C. Xuan, G. Liu, Z. Chen, W. Wang, A label-free fluorescent biosensor for determination of bovine serum albumin and calf thymus DNA based on gold nanorods coated with acridine orange-loaded mesoporous silica, Sensors and Actuators B: Chemical 220 (2015) 302-308.

[80] V.K. Verma, K. Tapadia, T. Maharana, A. Sharma, Convenient and ultra-sensitive fluorescence detection of bovine serum albumin by using Rhodamine-6G modified gold nanoparticles in biological samples, Luminescence 33(8) (2018) 1408-1414.

[81] S. Ge, J. Lu, M. Yan, F. Yu, J. Yu, X. Sun, Fluorescence resonance energy transfer sensor between quantum dot donors and neutral red acceptors and its detection of BSA in micelles, Dyes and Pigments 91(3) (2011) 304-308.

[82] H.-J. Chen, Z.-H. Zhang, L.-J. Luo, S.-Z. Yao, Surface-imprinted chitosan-coated magnetic nanoparticles modified multi-walled carbon nanotubes biosensor for detection of bovine serum albumin, Sensors and Actuators B: Chemical 163 (2012) 76- 83.

[83] C. Guoning, G. Pengqi, W. Yan, W. Lu, S. Hua, L. Yunzhe, J. Wanghui, C. Chun, F. Qiang, Preparation of molecularly imprinted polymers and application in a biomimetic biotin-avidin-ELISA for the detection of bovine serum albumin, Talanta (2019).

[84] Q.-Q. Gai, F. Qu, T. Zhang, Y.-K. Zhang, The preparation of bovine serum albumin surface-imprinted superparamagnetic polymer with the assistance of basic functional monomer and its application for protein separation, Journal of Chromatography A 1218(22) (2011) 3489-3495.

[85] N. Elahi, M. Kamali, M.H. Baghersad, Recent biomedical applications of gold nanoparticles: a review, Talanta (2018).

[86] P.M. Tiwari, K. Vig, V.A. Dennis, S.R. Singh, Functionalized gold nanoparticles and their biomedical applications, Nanomaterials 1(1) (2011) 31-63.

[87] N. Chamuah, A. Saikia, A.M. Joseph, P. Nath, Blu-ray DVD as SERS substrate for reliable detection of albumin, creatinine and urea in urine, Sensors and Actuators B: Chemical (2019).

[88] E. Petryayeva, U.J. Krull, Localized surface plasmon resonance: nanostructures, bioassays and biosensing—a review, Analytica chimica acta 706(1) (2011) 8-24.

[89] A. Yari, M. Saeidikhah, Ultra-trace electrochemical impedance determination of bovine serum albumin by a two dimensional silica network citrate-capped gold nanoparticles modified gold electrode, Talanta 144 (2015) 1336-1341.

[90] D. Duan, H. Yang, Y. Ding, D. Ye, L. Li, G. Ma, Three-dimensional molecularly imprinted electrochemical sensor based on Au NPs@Ti-based metal-organic frameworks for ultra-trace detection of bovine serum albumin, Electrochimica Acta 261 (2018) 160-166.

[91] R. Viter, I. Iatsunskyi, V. Fedorenko, S. Tumenas, Z. Balevicius, A. Ramanavicius, S. Balme, M. Kempiński, G. Nowaczyk, S. Jurga, Enhancement of electronic and optical properties of ZnO/Al_2O_3 nanolaminate coated electrospun nanofibers, The Journal of Physical Chemistry C 120(9) (2016) 5124-5132.

[92] Y. Zhang, T. R Nayak, H. Hong, W. Cai, Biomedical applications of zinc oxide nanomaterials, Current molecular medicine 13(10) (2013) 1633-1645.

[93] A. Sanginario, V. Cauda, A. Bonanno, K. Bejtka, S. Sapienza, D. Demarchi, An electronic platform for real-time detection of bovine serum albumin by means of amine-functionalized zinc oxide microwires, RSC Advances 6 (2016) 891-897.

[94] M. Sasmal, T.K. Maiti, T.K. Bhattacharyya, Synthesis of ZnO nanosphere for picomolar level detection of bovine serum albumin, IEEE transactions on nanobioscience 14(1) (2015) 129-137.

[95] Z. Balevicius, A. Paulauskas, I. Plikusiene, L. Mikoliunaite, M. Bechelany, A. Popov, A. Ramanavicius, A. Ramanaviciene, Towards the application of Al_2O_3/ZnO nanolaminates in immunosensors: total internal reflection spectroscopic ellipsometry based evaluation of BSA immobilization, Journal of Materials Chemistry C 6(32) (2018) 8778-8783.

[96] X.-H. Yang, J. Ling, J. Peng, Q.-E. Cao, L. Wang, Z.-T. Ding, J. Xiong, Catalytic formation of silver nanoparticles by bovine serum albumin protected-silver nanoclusters and its application for colorimetric detection of ascorbic acid, Spectrochimica Acta Part A: Molecular and Biomolecular Spectroscopy 106 (2013) 224-230.

[97] H. Pan, X. Tao, C. Mao, J.-J. Zhu, F. Liang, Aminopolycarboxyl-modified Ag2S nanoparticles: Synthesis, characterization and resonance light scattering sensing for bovine serum albumin, Talanta 71(1) (2007) 276-281.

[98] K. Kamakshi, J. Silva, K. Sekhar, G. Marslin, J.A. Moreira, O. Conde, A. Almeida, M. Pereira, M. Gomes, Influence of substrate temperature on the properties of pulsed laser deposited silver nanoparticle thin films and their application in SERS detection of bovine serum albumin, Applied Physics B 122(5) (2016) 108.

[99] L.L. Zhang, F.F. Ma, Y.F. Kuang, S. Cheng, Y.F. Long, Q.G. Xiao, Highly sensitive detection of bovine serum albumin based on the aggregation of triangular silver nanoplates, Spectrochimica Acta Part A: Molecular and Biomolecular Spectroscopy 154 (2016) 98-102.

[100] L.B. Devi, S. Berchmans, A.B. Mandal, Highly sensitive detection of proteins using voltammetric assay in the presence of silver nanostructures, Journal of Electroanalytical Chemistry 665 (2012) 20-25.

[101] M.J. Allen, V.C. Tung, R.B. Kaner, Honeycomb carbon: a review of graphene, Chemical reviews 110(1) (2009) 132-145.

[102] Y. Ni, F. Zhang, S. Kokot, Graphene oxide as a nanocarrier for loading and delivery of medicinal drugs and as a biosensor for detection of serum albumin, Analytica chimica acta 769 (2013) 40-48.

[103] I.V. Zaporotskova, N.P. Boroznina, Y.N. Parkhomenko, L.V. Kozhitov, Carbon nanotubes: Sensor properties. A review, Modern Electronic Materials 2(4) (2016) 95-105.

[104] M. Zhang, J. Huang, P. Yu, X. Chen, Preparation and characteristics of protein molecularly imprinted membranes on the surface of multiwalled carbon nanotubes, Talanta 81(1-2) (2010) 162-166.

[105] B.B. Prasad, A. Prasad, M.P. Tiwari, Multiwalled carbon nanotubes-ceramic electrode modified with substrate-selective imprinted polymer for ultra-trace detection of bovine serum albumin, Biosensors and Bioelectronics 39(1) (2013) 236-243.

[106] J.M. Klostranec, W.C. Chan, Quantum dots in biological and biomedical research: recent progress and present challenges, Advanced Materials 18(15) (2006) 1953-1964.

[107] M. Zhang, M. Yan, J. Yu, S. Ge, F. Wan, L. Ge, Monitoring of bovine serum albumin using ultrasensitive electrochemiluminescence biosensors based on multilayer CdTe quantum dots modified indium tin oxide electrodes, Analytical Methods 4(2) (2012) 460-466.

[108] Y. Yu, Y. Lai, X. Zheng, J. Wu, Z. Long, C. Liang, Synthesis of functionalized CdTe/CdS QDs for spectrofluorimetric detection of BSA, Spectrochimica Acta Part A: Molecular and Biomolecular Spectroscopy 68(5) (2007) 1356-1361.

[109] Y.-Q. Yang, X.-W. He, Y.-Z. Wang, W.-Y. Li, Y.-K. Zhang, Epitope imprinted polymer coating CdTe quantum dots for specific recognition and direct fluorescent quantification of the target protein bovine serum albumin, Biosensors and Bioelectronics 54 (2014) 266-272.

[110] P. Kumar, A. Deep, S.C. Sharma, L.M. Bharadwaj, Bioconjugation of InGaP quantum dots for molecular sensing, Analytical biochemistry 421(1) (2012) 285-290.

[111] H.E. Indyk, B.D. Gill, D.C. Woollard, An optical biosensor-based immunoassay for the determination of bovine serum albumin in milk and milk products, International Dairy Journal 47 (2015) 72-78.

[112] M. Kukkar, A. Sharma, P. Kumar, K.-H. Kim, A. Deep, Application of MoS_2 modified screen-printed electrodes for highly sensitive detection of bovine serum albumin, Analytica chimica acta 939 (2016) 101-107.

[113] M. Chiku, T.A. Ivandini, A. Kamiya, A. Fujishima, Y. Einaga, Direct electrochemical oxidation of proteins at conductive diamond electrodes, Journal of Electroanalytical Chemistry 612(2) (2008) 201-207.

[114] C.-J. Cui, W.-S. Cai, X.-G. Shao, Near-infrared diffuse reflectance spectroscopy with sample spots and chemometrics for fast determination of bovine serum albumin in micro-volume samples, Chinese Chemical Letters 24(1) (2013) 67-69.

[115] Y. Cai, F. Yin, Q. Xie, Y. Zhang, S. Yao, The detection of bovine serum albumin by using Cu^{2+} based on a piezoelectric quartz crystal impedance technique, Microchemical journal 68(1) (2001) 71-76.

[116] J. de Paula Rezende, G.M.D. Ferreira, G.M.D. Ferreira, L.H.M. da Silva, M.d.C.H. da Silva, M.S. Pinto, A.C. dos Santos Pires, Polydiacetylene/triblock copolymer nanosensor for the detection of native and free bovine serum albumin, Materials Science and Engineering: C 70 (2017) 535-543.

Figure captions

Figure 1: The structure of HSA as displayed in the cartoon image which is mainly composed of three main domains namely as domains I, II and III, and each domain contains two subdomains A and B. There are two main binding sites on BSA namely as sites I and II which are located in the subdomains IIA and IIIA, respectively.

Figure 2: Synthesis of the target compound DPPAM (A). Attachment of 1, 4-dibromobutane to DPP core and the formation of compound 2. Cross-coupling reaction between compound 2 and 4-(bis(4-methoxyphenyl)-amino) phenylboronic acid and preparation of compound 3. Treatment of compound 3 with TMA in THF and obtainment of DPPAM. Illustration of the fluorescence turn-on sensor for BSA detection based on the AIE properties of the synthesized DPPAM (B). DPPAM showed a sharp increase in NIR emissions due to electrostatic interactions between the ammonium groups of DPPAM and BSA [39].

Figure 3: The chemical structures of DPP1 and DPP2 probes and their synthesis route. Compound 5 was synthesized in five steps using *p*-cyanobenzaldehyde as starting material. DPP1andDPP2 probes were synthesized by the reaction of diethylamine and trimethylamine with compound 5, respectively [68].

Figure 4: Schematic illustration of BSA detection using the hybrid of Cys3 dye and CCG. Cy3 dye fluorescence intensity is considerably reduced due to its interaction with CCG. In the presence of BSA, the fluorescence intensity of Cy3 enhances which is proportional to the albumin concentrations [70].

Figure 5: The chemical structures of SQ (A), ruthenium (II) complexes I and II (B), CIHARP (C), 9, 10-anthraquinone (D), Nile blue (E), DISA along with its preparation route (F), and enoxacin (G).

Figure 6: Schematic representations for BSA determination using the energy transfer between R6G and AuNPs (A). The fluorescence of R6G dyes is quenched by AuNPs. However, upon the addition of BSA, the interacted dyes are released from the surface of AuNPs, and the fluorescence intensity is proportional to the amount of the added albumin [80]. BSA detection using CdTe QDs and NR dye as illustrated in a schematic image (B). The interaction of CdTe QDs and NR in micelles caused to decrease the fluorescence intensity resulting from FRET-based energy transfer, and BSA addition recovered the fluorescence emission upon releasing the interacted dyes from the surface of QDs [81].

Figure 7: A graphic schemes for the fabrication of the proposed electrode using Au NPs and the sensing processes for the determination of BSA [89].

Figure 8: The proposed reaction mechanism for EDC/sulfo-NHS/BSA-NH_2. Interaction of only bi-distilled water with the ZnO microwire and the parallel capacitance slightly increase at the electrodes (A); the formation of an electrical double layer on the electrode and increase the capacitance after the addition of EDC and sulfo-NHS without the effect on ZnO microwire (B); creation of amine-reactive intermediate compounds after the addition of BSA via the EDC/sulfo-NHS reaction (C); the increase of ZnO capacitance upon the reaction of the intermediate with ZnO amine groups and BSA binding via carboxyl group to the ZnO microwire (D); continuation of the increase of capacitance until the full saturation of all ZnO reaction sites (E) [93].

Figure 9: The interaction mechanism of HCPT, BSA, and GO which has been considered for the determination of BSA [102].

Figure 10: Schematic diagram of LbL self-assembled processes of multilayer QDs films. The preparation procedure can be shown in three main steps: preparation of APS layer using APS; fabrication of capped CdTe QDs on an ITO by TGA; LbL self-assembly of CdTe QDs on the modified ITO glass (A) [107]. EDC-NHS mediated bioconjugation of anti-BSA with InGaP QDs (B) [110].

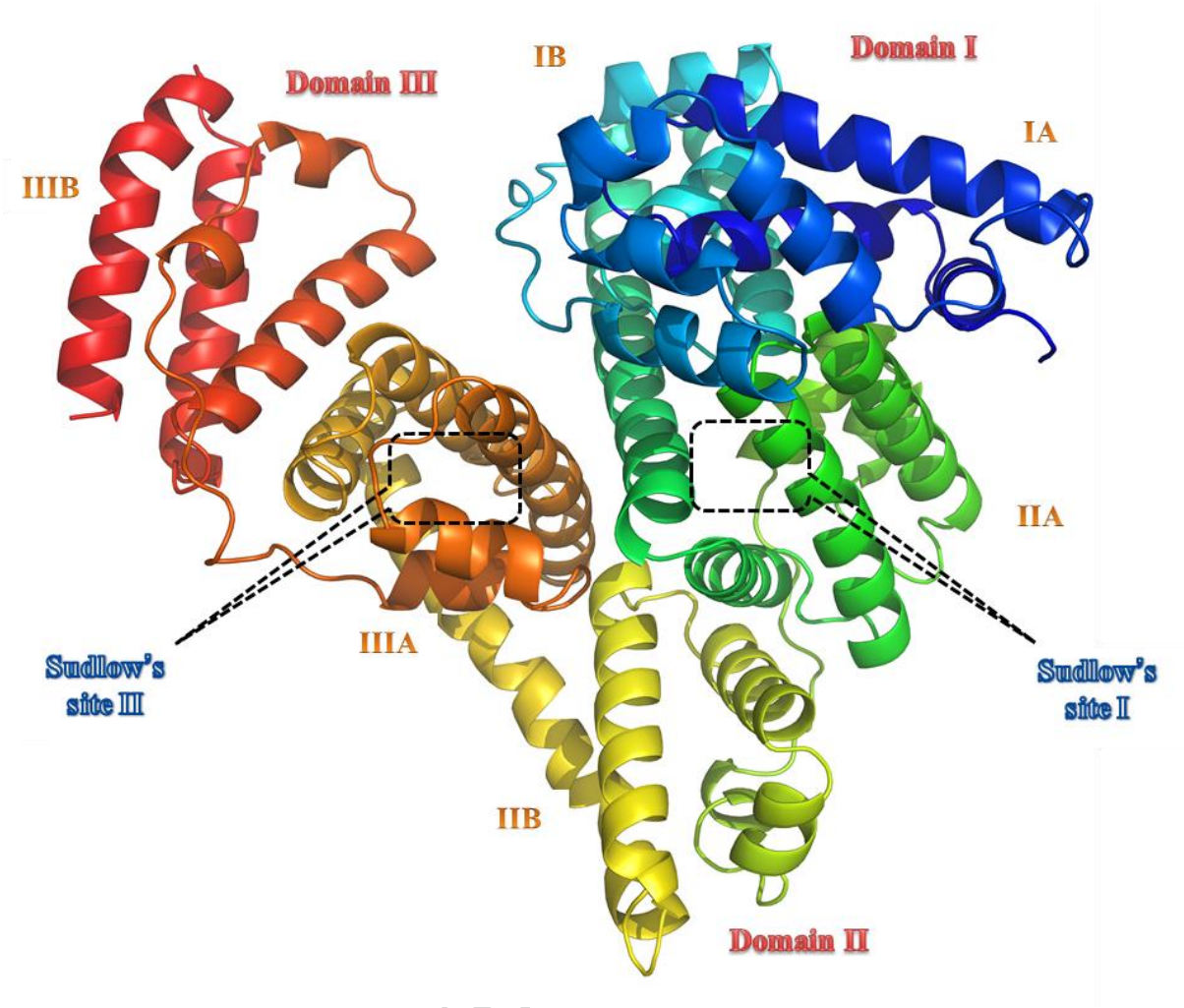

Figure 1

(A)

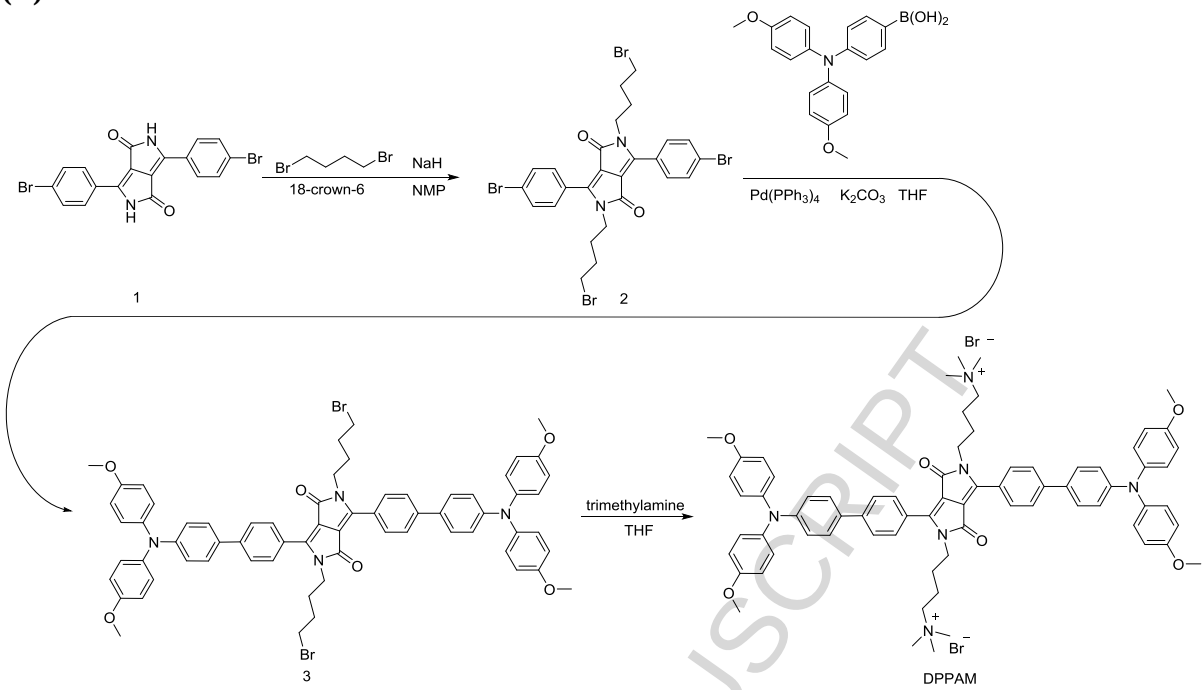

(B)

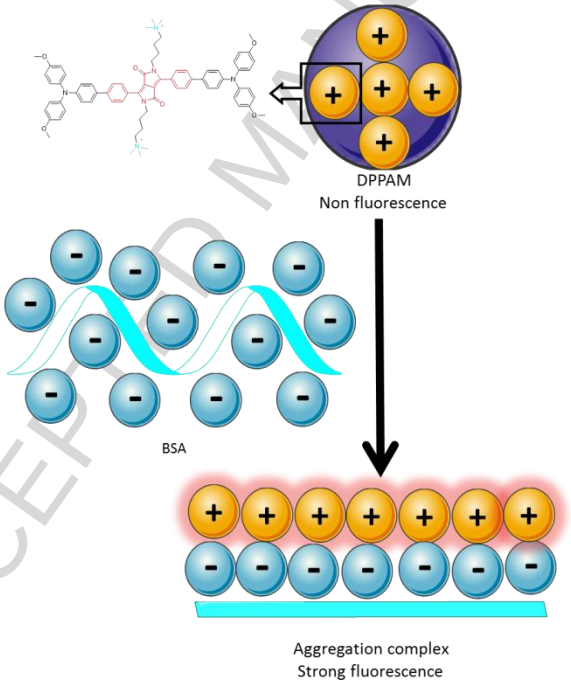

Figure 2

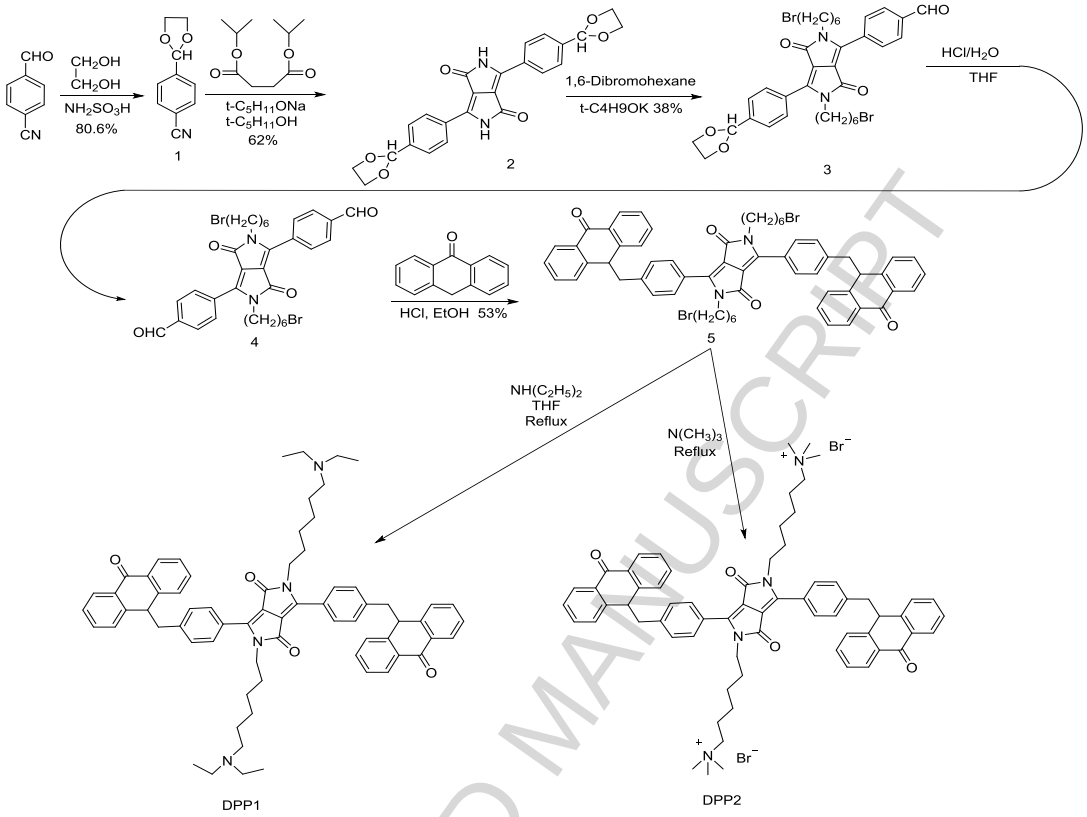

Figure 3

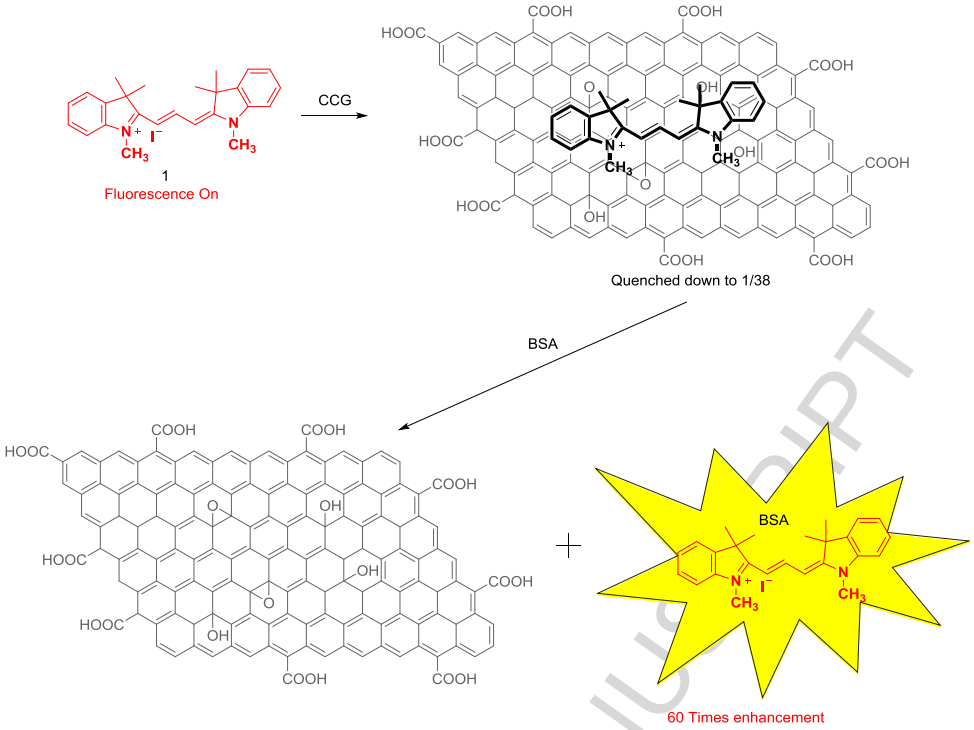

Figure 4

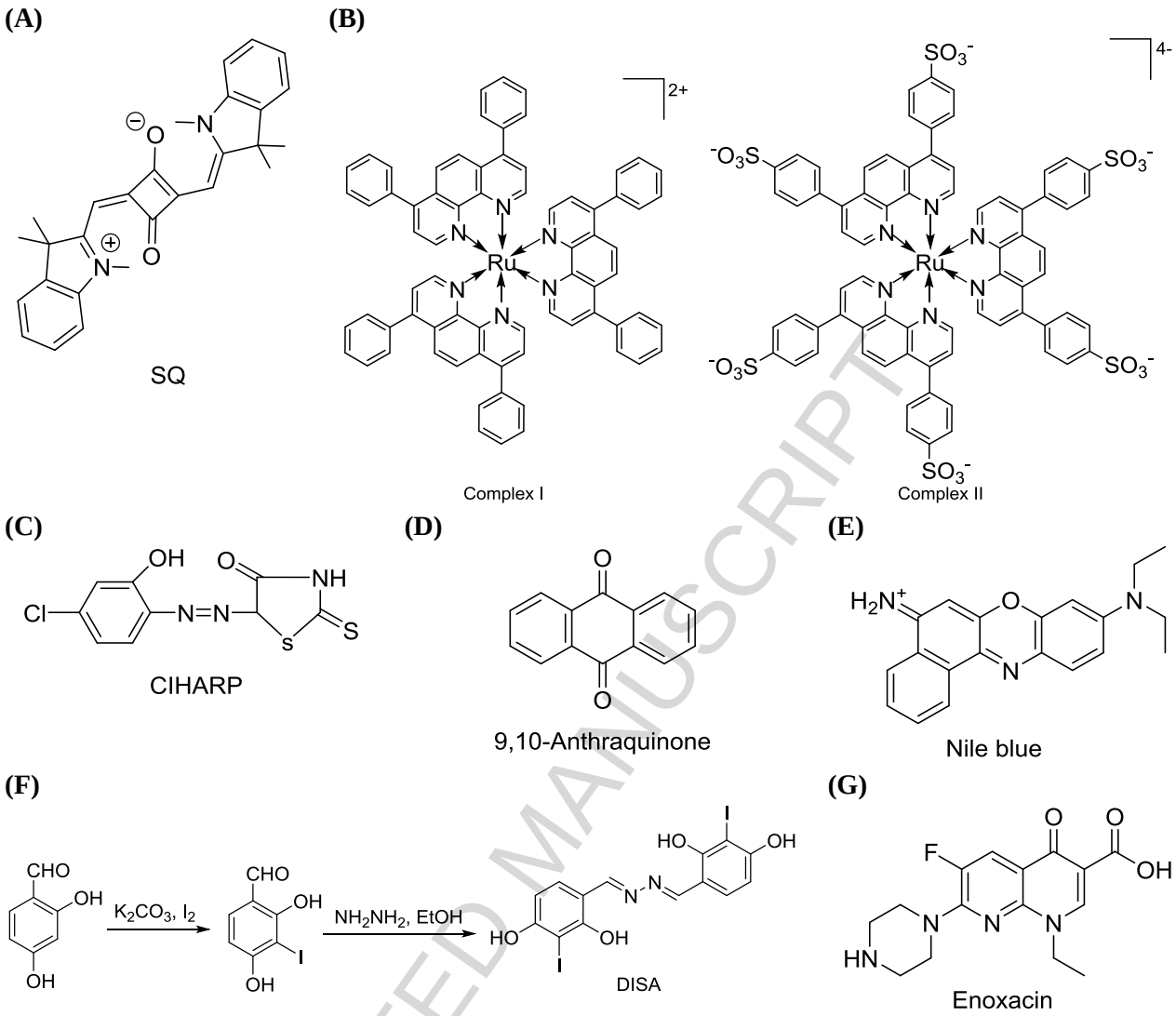

Figure 5

(A)

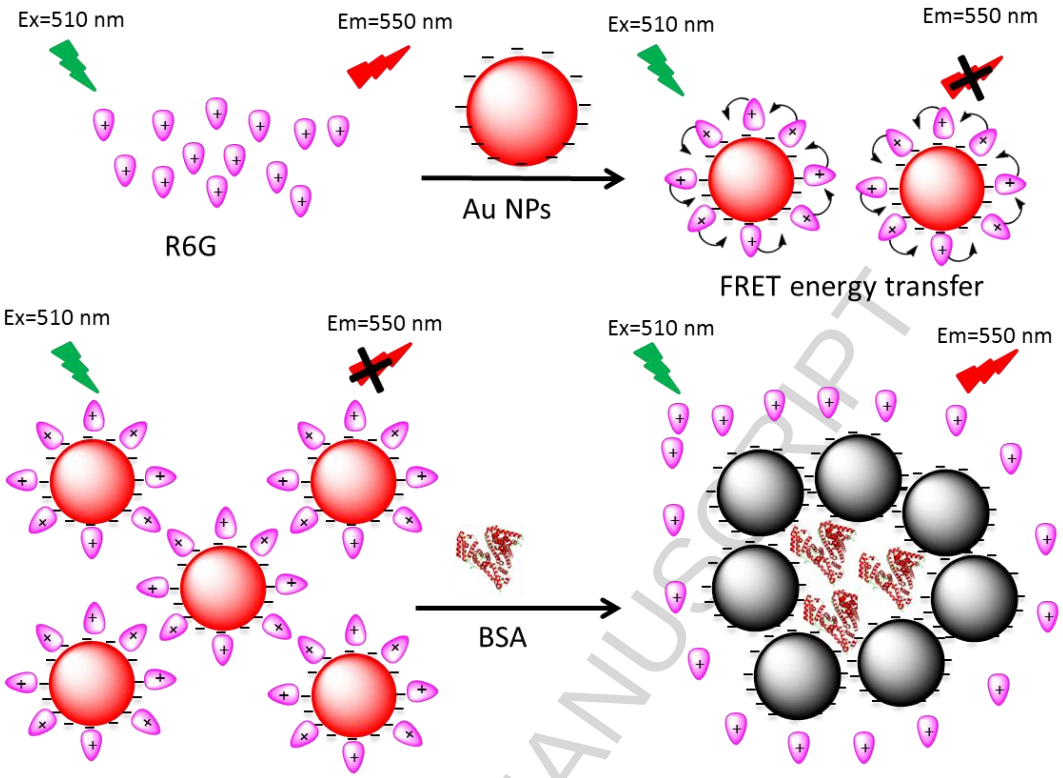

(B)

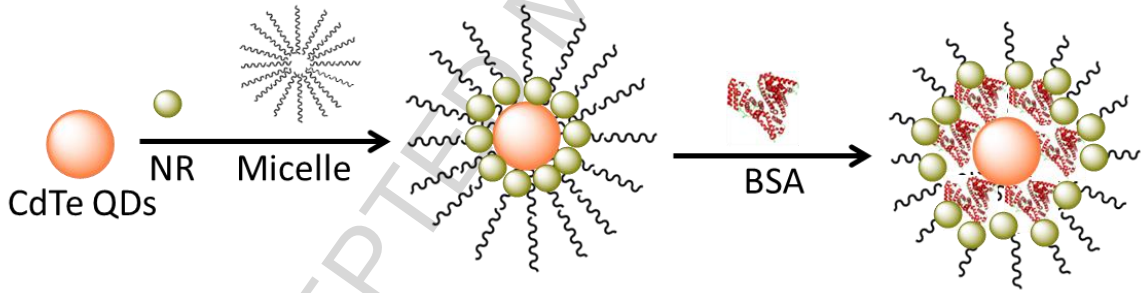

Figure 6

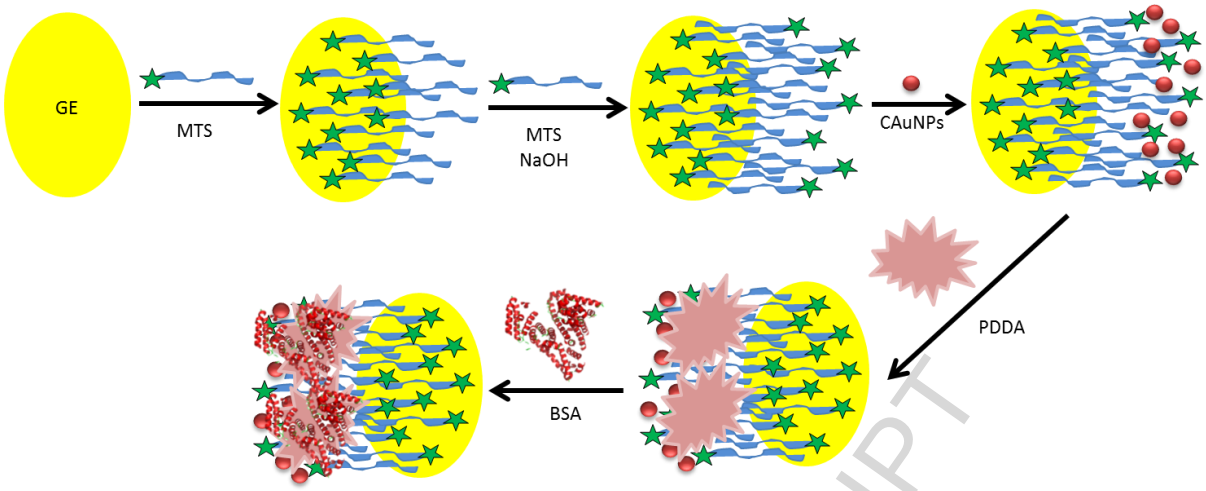

Figure 7

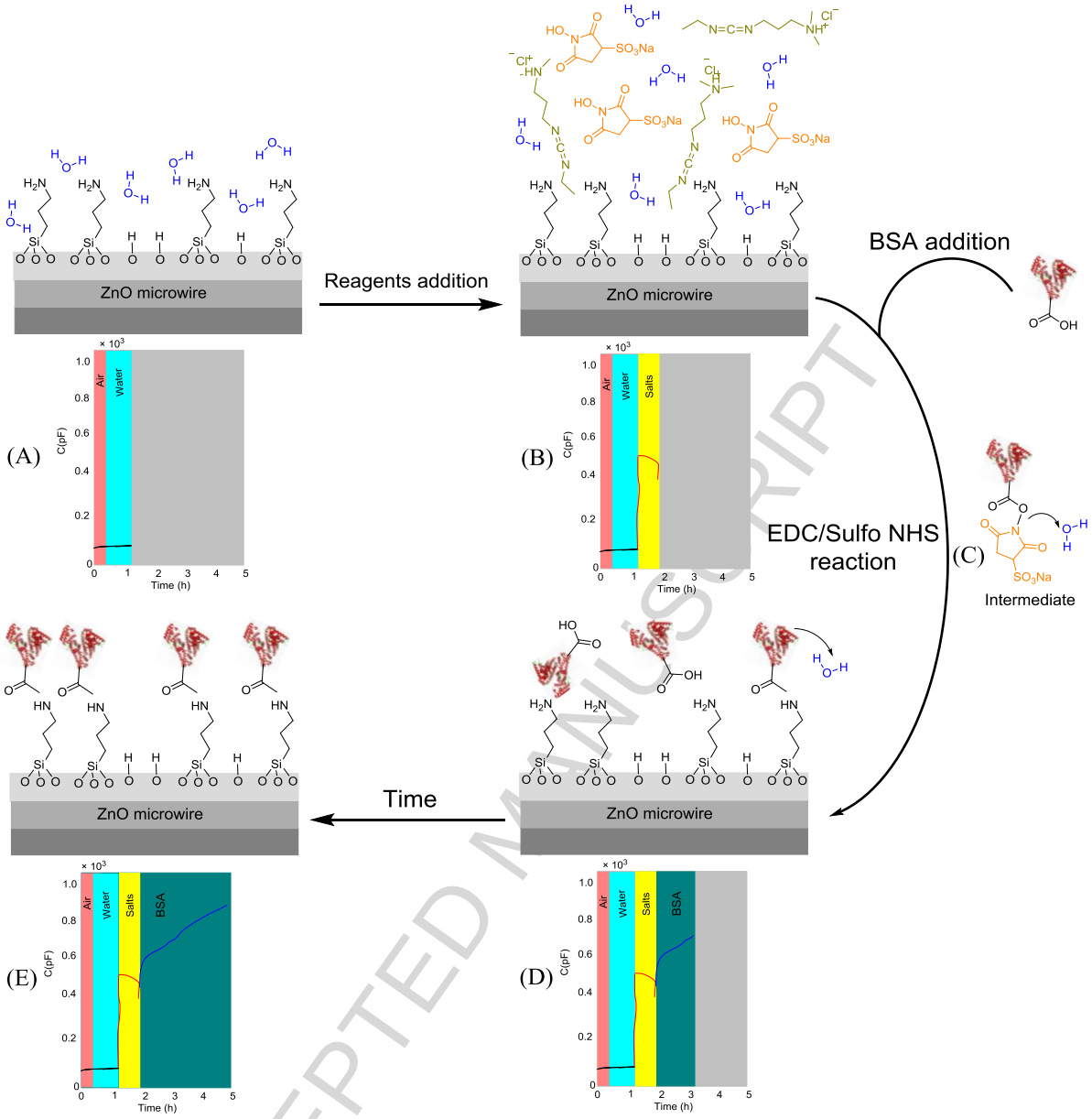

Figure 8

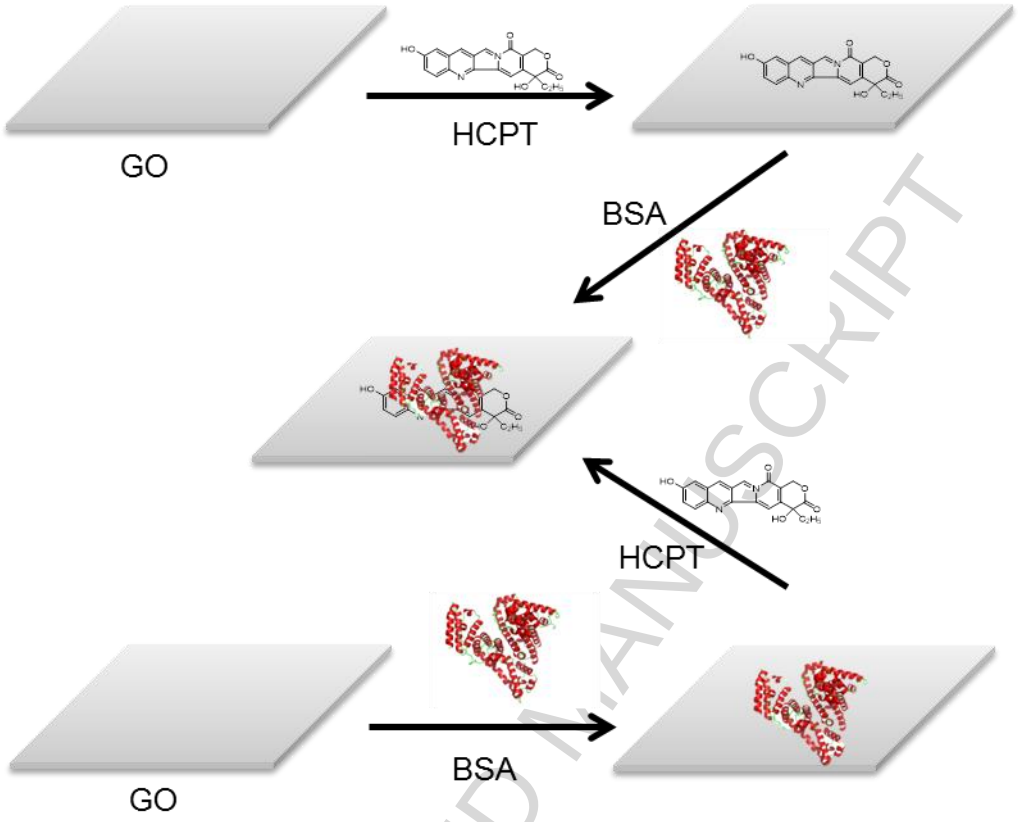

Figure 9

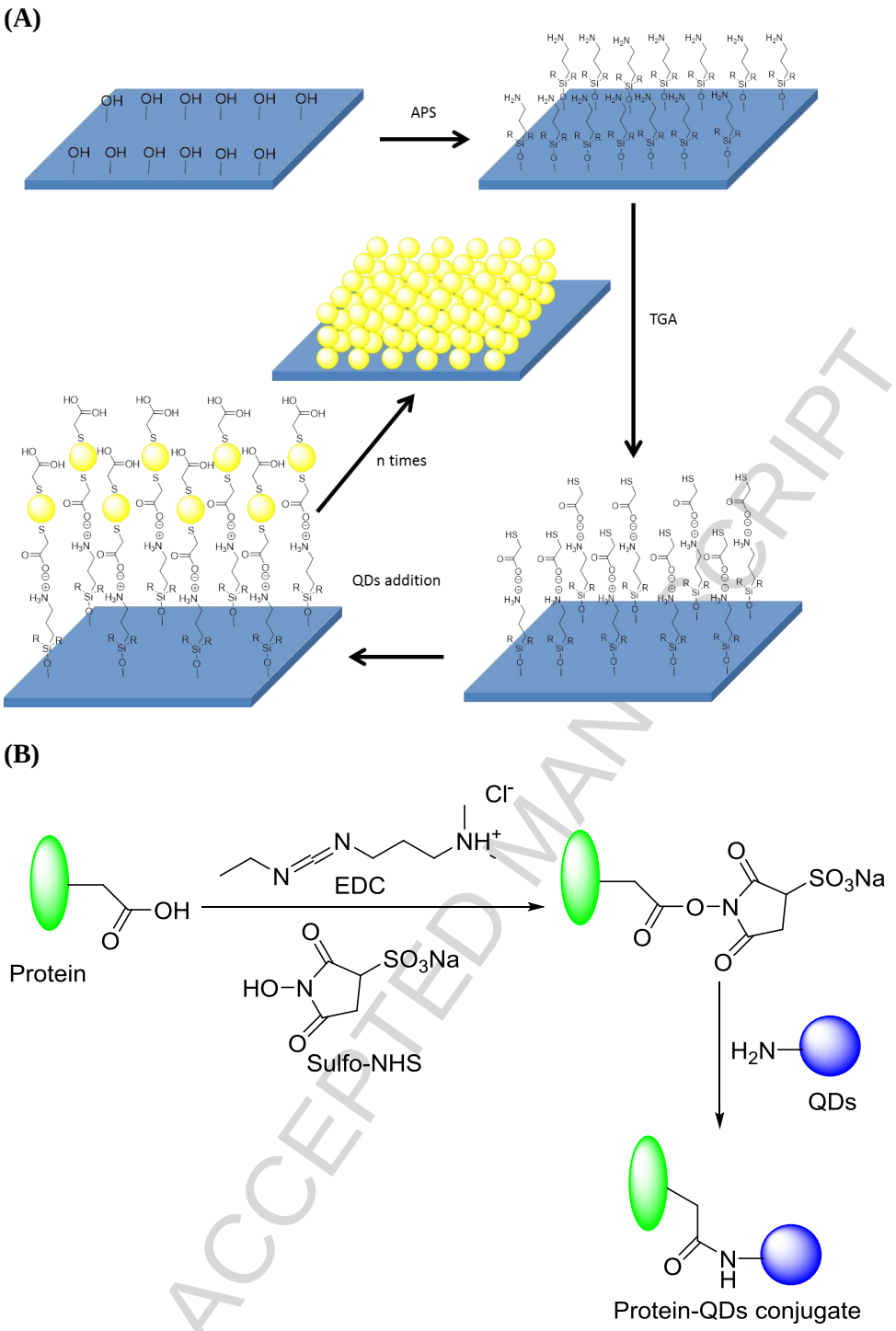

Figure 10